

disrupted, allowing a foothold for regeneration taxa. The absence of altitudinally-restricted taxa during some probable stadials could indicate that there was a lag in the migration of many species during episodes of rapid temperature change, but many taxa seem to have been able to migrate extremely rapidly.

There is a range of evidence that people actively managed vegetation using fire to create forest-edge habitats during interstadials, from the beginning of the known sequence *c.* 53,000 years ago, and that this pattern persisted in the Holocene until at least 6500 years ago at Loagan Bunut, and probably into sub-recent

times at Niah. This provides a partial explanation of how people could colonize and use tropical forest environments during the Late Pleistocene. During the Holocene, the management of vegetation seems to have been transformed into a system involving sago palms and rice, contemporary with if not earlier than the precocious agriculture based on bananas and tuberous plants known from New Guinea (Denham 2011; Denham *et al.* 2003, 2004; Haberle *et al.* 2012), ancient practices that were still present in Borneo until the recorded past and that may survive in some form today.

Chapter 9

Stable Isotope Analysis of Shells from the West Mouth: Palaeoenvironments, Seasonality and Harvesting

Mark Stephens with James Rose, David Matthey and David Gilbertson

Introduction

Elements such as oxygen and carbon contain isotopes that have the same chemical properties but different atomic masses, the difference in weight causing 'fractionation' in the course of certain chemical and physical processes occurring in nature. For example, during glacial periods when large ice masses built up over the Northern Hemisphere, there was a preferential removal of the lighter oxygen isotope from oceans and air masses (Shackleton 1987), leading to a concentra-

tion or enrichment of the heavier oxygen isotope in the oceans ($H_2^{18}O$) and a subsequent increase of the lighter isotope ($H_2^{16}O$) in ice masses as recorded in ice cores (e.g. Dansgaard *et al.* 1993). Isotope studies of past climates are well established in the northern latitudes but far less developed in the humid tropics, particularly of Southeast Asia. Hence one component of the NCP was an investigation of the isotopic ratios in mollusc shells from archaeological contexts in the West Mouth held in the Harrison Excavation Archive (Fig. 9.1), compared with studies of modern shells undertaken

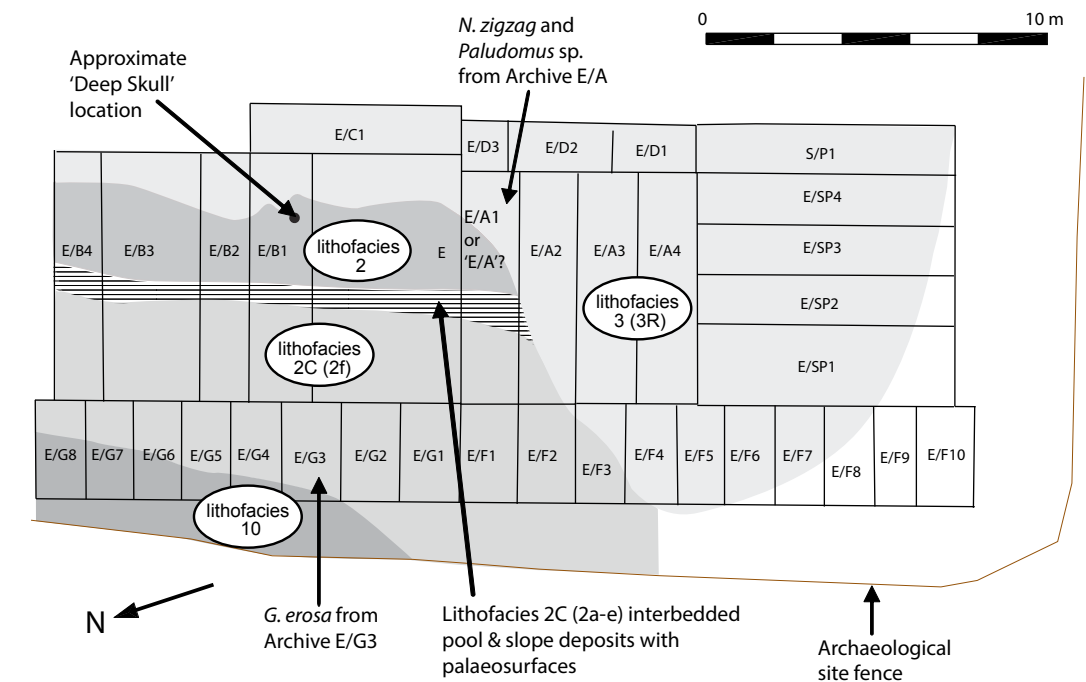


Figure 9.1. The layout of some of the main Harrison trenches in the Hell Trench of the West Mouth, with the approximate likely location of the Deep Skull and the lithofacies defined by the NCP (Gilbertson *et al.* 2005; and see Volume One, Chapter 3, and this volume, Chapter 5), and the locations of the mollusc shells sampled from the Harrison Excavation Archive.

to understand the isotopic systematics of the modern environment around the caves (Stephens & Rose 2005), as a means of gaining information about the climatic regimes in which the molluscs lived and the seasons in which they were collected (Andrus & Crowe 2000; Bailey *et al.* 1983; Deith 1983, 1985; Deith & Shackleton 1988; Godfrey 1988; Kennett & Voorhies 1996; Killingley 1981, 1983; Mannino *et al.* 2003; Shackleton 1969, 1973). The archaeological shells in the Archive are thought to have been collected variously a food source, a decorative medium, and as tools (Medway 1960a; and see [this volume, Chapters 19 and 28](#)).

Palaeoenvironmental reconstruction from mollusc shells using stable isotopes

Of the mollusc shells found in the West Mouth, the Bivalvia and Gastropoda classes are dominant. In Bivalvia the body is encased in a shell containing two valves hinged together, the valve growing outwards from the umbo to the ventral margin (Fig. 9.2a). In Gastropoda the body is within a coiled shell that grows in a spiralled tube from the apex to the aperture (Fig. 9.2b). It is this accretionary growth that provides the environmental record through time (Rhoads & Lutz 1980). Most bivalves and gastropods grow by addition of material at the outer margin of the valves and aperture respectively and can produce several layers of material including the outer organic periostracum and inner shell layers. The periostracum isolates the shell edge during calcification and protects the shell from dissolution in acidic waters (Wilbur & Saleuddin 1983). Molluscs generally produce aragonitic or calcitic shells, or use both mineralogies to make their shell based on adaptive and evolutionary processes (Carter 1980).

It has been demonstrated through analysis of modern shells and the surrounding environment, including laboratory culturing under known environmental conditions, that the shell chemistry of molluscs represents a record of environmental parameters (Dodd 1965; Hickson *et al.* 1999; Khim *et al.* 2000; Klein *et al.* 1996a, 1996b; Krantz *et al.* 1987; Lazareth *et al.*

2003; Ricken *et al.* 2003; Surge *et al.* 2003; Vander Putten *et al.* 2000; Wurster & Patterson 2001). In Sarawak, for example, freshwater molluscs (*Brotia costula*, *Melanoides tuberculata* and *Clithon* sp.) have been used as indicators of heavy metal accumulation from gold mining pollution in the Sungai Sarawak Kanan that flows into Kuching (Lau *et al.* 1998). As a result, the successively deposited shell calcium carbonate layers are potential archives of the varying environmental conditions that the mollusc has experienced during its life (Hart & Blusztajn 1998; Klein *et al.* 1996a, 1996b; Leng & Pearce 1999; Pannella & MacClintock 1968; Richardson 2001; Surge *et al.* 2003). In his analysis of microgrowth patterns in the modern intertidal and subtidal Malaysian bivalve *Anadara granosa*, Richardson (1987) found growth bands with a tidal and monsoonal periodicity of formation. Less isotopic research has been carried out on estuarine and freshwater shells mainly due to a greater complexity of factors affecting the oxygen and carbon stable isotopic fractionation processes, but useful palaeoenvironmental reconstructions include studies of palaeosalinity (e.g. Ingram *et al.* 1996), palaeomonsoon (e.g. Abell *et al.* 1995) and palaeohumidity (e.g. Schmitz & Andreasson 2000).

Both theoretical calculations (Urey 1947) and experiments (Epstein *et al.* 1953; Grossman & Ku 1986; Kim & O'Neil 1997; McCrea 1950; O'Neil *et al.* 1969) have shown that the $\delta^{18}\text{O}$ of a slowly precipitating carbonate is controlled both by the $\delta^{18}\text{O}$ of the water in which precipitation occurs and the water temperature. In the marine setting, the isotopic composition of the water remains relatively constant and so palaeotemperature reconstructions from marine shells are fairly accurate. Riverine and especially estuarine environments, however, have more interacting factors affecting the stable isotopic composition of the water: the stable isotopic signal of rainfall, evaporation, residence time, groundwater contribution and exchange with seawater in the estuarine zone (Stephens & Rose 2005; Fig. 9.3).

In wet tropical areas where seasonal temperature changes are minimal, the heavy rainfalls control fractionation of ^{18}O and ^{16}O , the stable isotopes of oxygen

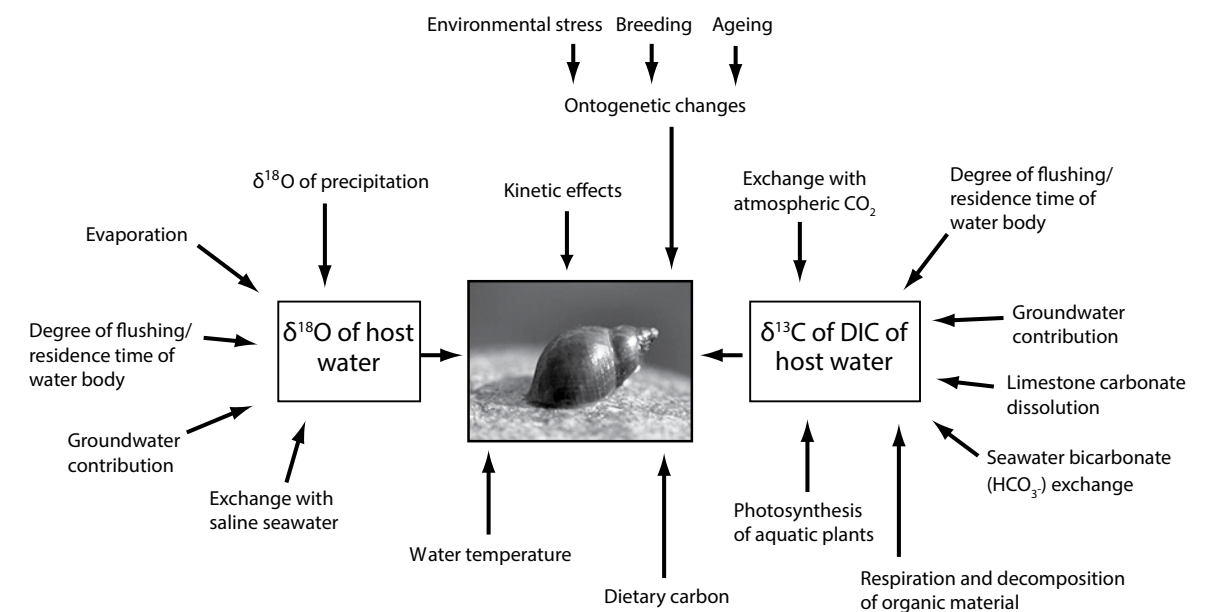


Figure 9.3. Natural environmental factors affecting carbon and oxygen isotopes in riverine and estuarine molluscs of the Niah River (Sunghai Niah) catchment.

(Araguás-Araguás *et al.* 1998; Dansgaard 1964; Gat 1996). Source and transport history of rains are also important factors (e.g. Aggarwal *et al.* 2004). Major moisture sources for Sarawak during the winter monsoon are the tropical western Pacific Ocean and the South China Sea, whereas moisture from the Indian Ocean dominates during the summer monsoon. Stable isotope analysis of dated groundwaters in South and Southeast Asia suggests that the overall structure of monsoon circulation and moisture transport patterns have remained relatively stable over the last 20,000 years (Aggarwal *et al.* 2004). This body of observation suggests that there is potential in the wet lowland tropics for both the reconstruction of the isotopic composition of the water that the mollusc used to grow its shell, and to make inferences about previous monsoon rainfall conditions (e.g. Kennett & Voorhies 1995).

Studies of carbon isotopes provide useful information such as about biological cycling within the drainage catchment (e.g. Keith & Parker 1965; Keith *et al.* 1964), vegetation type (C3 vs. C4 plants: e.g. Surge *et al.* 2003) and diet (e.g. Metref *et al.* 2003), depending on what carbon source the mollusc used to build its shell. The carbon sources for aquatic molluscs are dissolved inorganic carbon (DIC) and/or metabolic carbon. Fritz and Poplawski (1974) and Hickson *et al.* (1999) report DIC as the primary control of shell $\delta^{13}\text{C}$, but Tanaka *et al.* (1986) showed that up to 85% of mollusc shell carbonate can originate from

metabolic carbon. Indeed, where a large negative shift exists in $\delta^{13}\text{C}$ shell relative to the DIC, metabolic CO_2 derived from respiration is commonly attributed as a major factor (e.g. Dettman *et al.* 1999; Fastovsky *et al.* 1993; Mueller-Lupp *et al.* 2003; Owen *et al.* 2002; Vander Putten *et al.* 2000). Linked to changes in the metabolism of a mollusc are ontogenetic factors such as feeding, growth, old age and reproductive activity (Erlenkeuser & Wefer 1981; Krantz *et al.* 1987; Vander Putten *et al.* 2000; Wefer & Berger 1991). Consequently, shell $\delta^{13}\text{C}$ variations might be influenced primarily by metabolism rather than reflect the carbon isotopic trend of DIC in the external aquatic environment. Hu *et al.* (2002) have demonstrated the dominant presence of C3 plants throughout the glacial and Holocene periods for north Borneo.

Another potential factor affecting stable isotopic signals in molluscs are post-burial diagenetic effects, of particular concern in the humid-tropical context where weathering and alteration of materials are most pronounced. Medway (1960a, 373) observed that shell preservation was poorer and depth of total dissolution much shallower in the damp peripheral trenches of the West Mouth than in the drier, more central, trenches. The micromorphology of the West Mouth sediments has evidence for localized down-profile transport of clays and minerals in solution, and weathering at the periphery of rock fragments (Stephens 2004a; Stephens *et al.* 2005; and [this volume, Chapter 5](#)). In the present

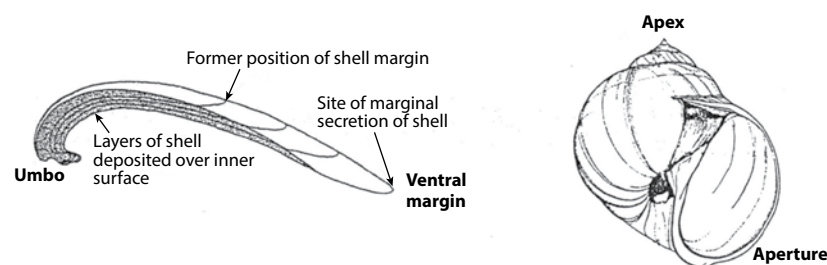


Figure 9.2 (left) Section through a generalized bivalve showing shell production from the umbo to the ventral margin; (right) sketch of a gastropod with typical helical shell growth from the apex to the aperture.

study X-Ray Diffraction (XRD), which can test for diagenetic alteration of shells (e.g. conversion from aragonite to its more stable polymorph calcite), was used to confirm the preservation of shell mineralogy.

Stable isotopes and the hydrological cycle in the tropics

In the global climate system the tropics are paramount for the transfer of moisture and heat to the higher latitudes and the maintenance of a climatic equilibrium. Tropical rainforest ecosystems are also an important global store (Dixon *et al.* 1994) and possible sink for carbon (Hashimoto *et al.* 2000; Phillips *et al.* 1998). River estuaries form a pathway linking the supply from the continent to the marine and atmospheric system (Frankignoulle *et al.* 1998; Richey *et al.* 2002). Tropical coastal ecosystems can undergo rapid and important changes tuned by the monsoon regimes and freshwater inputs can significantly modify environmental parameters such as salinity (Kitheka, 1996, 1998; Osore *et al.* 1997) and nutrient concentrations (Kazungu *et al.* 1989). The tropical hydrological component of the global cycling of water and carbon is, however, poorly understood. This diminishes our understanding of large-scale perturbations to the climate system (Chahine 1992), the development of valid global climate models (e.g. Henderson-Sellers *et al.* 2002) and the calibration of palaeoclimate proxies to modern systematics for the reconstruction of past environments (e.g. Stephens 2004a; Stephens & Rose 2005).

The selective fractionation of stable isotopes of oxygen ($^{18}\text{O}/^{16}\text{O}$), hydrogen ($^2\text{H}/^1\text{H}$) and carbon ($^{13}\text{C}/^{12}\text{C}$) within the natural environment permits an insight into the physical, chemical and biological cycling of H_2O and CO_2 . This information can be useful for evaluating globally-important processes such as rainforest evaporation budgets and the effects of deforestation (Martinelli *et al.* 1996), the description of atmospheric air mass circulation patterns (Njitchoua *et al.* 1999) and the recycling of continental moisture (Longinelli & Edmond 1983). The sources, fluxes and sinks of carbon can also be evaluated (Spiker 1980; Yang *et al.* 1996). In the tropics, however, such research has been limited so far to central and west equatorial Africa (e.g. Gonfiantini *et al.* 2001; Njitchoua *et al.* 1999), Central America (Lachniet & Patterson 2002) and the Amazon Basin (e.g. Longinelli & Edmond 1983; Martinelli *et al.* 1996; Quay *et al.* 1992). Stable isotope research in the tropics of Southeast Asia has been largely confined to the ongoing International Atomic Energy Agency/World Meteorological Organization Global Network 'Isotopes in Precipitation' project utilising isotopes of

oxygen and hydrogen (Araguás-Araguás *et al.* 1998). There is, however, no IAEA/WMO isotopic monitoring station in Borneo, so this study presents some of the first stable isotopic data ($\delta^{13}\text{C}$, $\delta^{18}\text{O}$, $\delta^2\text{H}$) reported from Borneo (Stephens & Rose 2005).

In the tropics of Southeast Asia there is a strong inverse relationship between mean monthly $\delta^{18}\text{O}$ and the amount of precipitation (Araguás-Araguás *et al.* 1998). This so-called 'amount effect' (Dansgaard 1964) is a powerful mechanism associated with the gradual rainout of moist, oceanic air masses moving inland forced by monsoon circulation, causing large isotopic depletions in rainfall. As rainout continues, the heavier ^{18}O isotopes are preferentially lost and so the rainfall becomes increasingly depleted. This process appears to be the main controlling factor throughout the tropical belt (e.g. Njitchoua *et al.* 1999) and has the effect of masking any dependence of $\delta^{18}\text{O}$ and $\delta^2\text{H}$ on temperature. The isotopic signal of an individual rainfall event is subsequently modified by the various fractionations and mixing of water bodies in its course from continental storage and eventual runoff into the sea (Fig. 9.4). Stable isotopic analysis of tropical aquatic mollusc shells therefore creates an opportunity to reconstruct ancient water regimes (e.g. Kennett & Voorhies 1995).

Craig (1961) sampled some 400 meteoric waters from around the world and, using the simple bi-plot of $\delta^2\text{H}$ vs. $\delta^{18}\text{O}$, produced a standard linear Global Meteoric Water Line (GMWL) that has a slope with a gradient of 8 and an intercept of 10 ($\delta^2\text{H} = 8 \cdot \delta^{18}\text{O} + 10$). An identical approximation was found by Rozanski *et al.* (1993), validating the work of Craig (1961). To put the Niah data in the regional context we compare our results against the Southeast Asia Regional Meteoric Water Line (RMWL) collated by Araguás-Araguás *et al.* (1998) from 61 stations in Southeast Asia and adjacent regions. The seasonal Southeast Asian RMWL varies from the GMWL, but when comparing annual data, the Southeast Asian RMWL is almost identical to the GMWL with a slope of 7.92 and intercept of 9.20, indicating that the relation observed by Craig (1961) and Rozanski *et al.* (1993) holds true.

Figure 9.5 shows schematically the important fractionation and mixing factors expected to affect the isotopic compositions of the hydrological carbon cycle at Niah. Natural water-dissolved inorganic carbon (DIC) consists of $\text{CO}_{2(\text{aq})}$, HCO_3^- and CO_3^{2-} . For any given stream, DIC can be influenced by contributions from groundwater, tributary streams, biogenic CO_2 uptake and release, or CO_2 invasion (Spiker 1980; Yang *et al.* 1996) and evasion (Aravena & Suzuki, 1990; Spiker 1980; Yang *et al.* 1996) from or to the atmosphere, subsequently affecting the carbon isotope

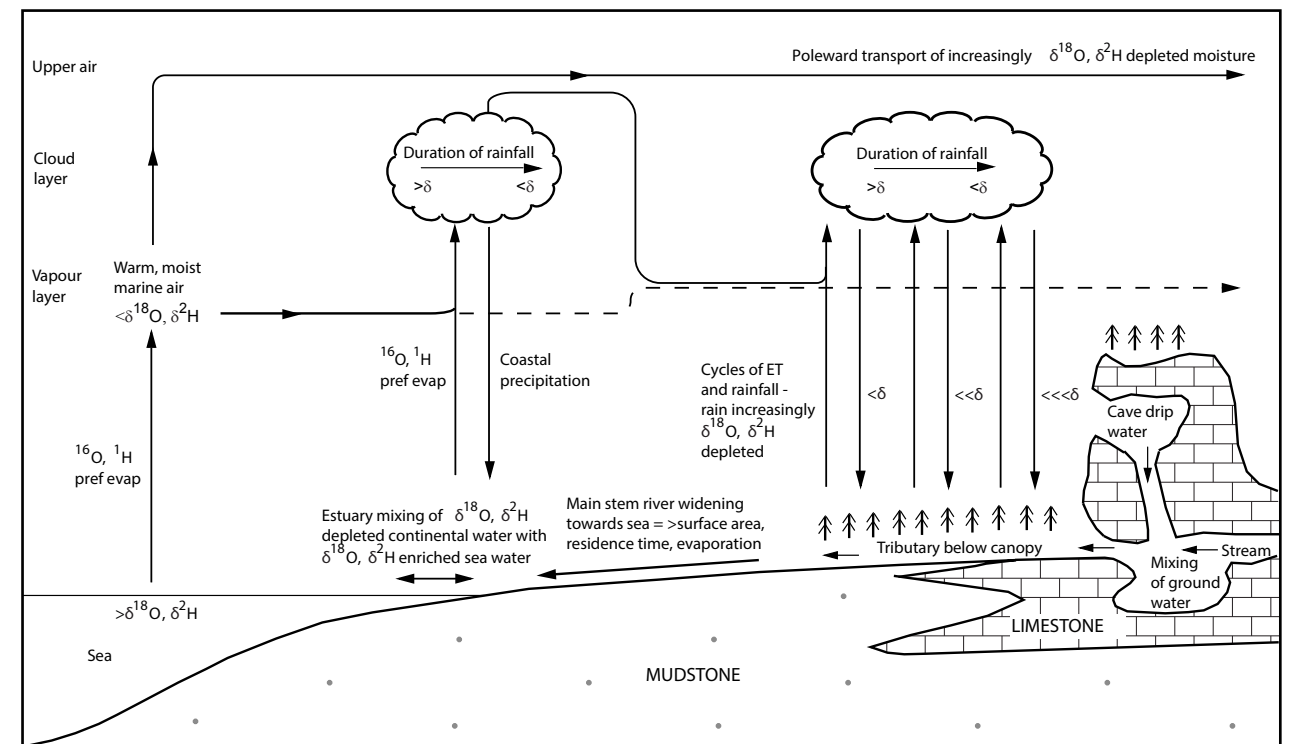


Figure 9.4. Schematic representation of $\delta^{18}\text{O}$ and $\delta^2\text{H}$ water cycling in the Niah River basin; partly adapted from Gat (1996).

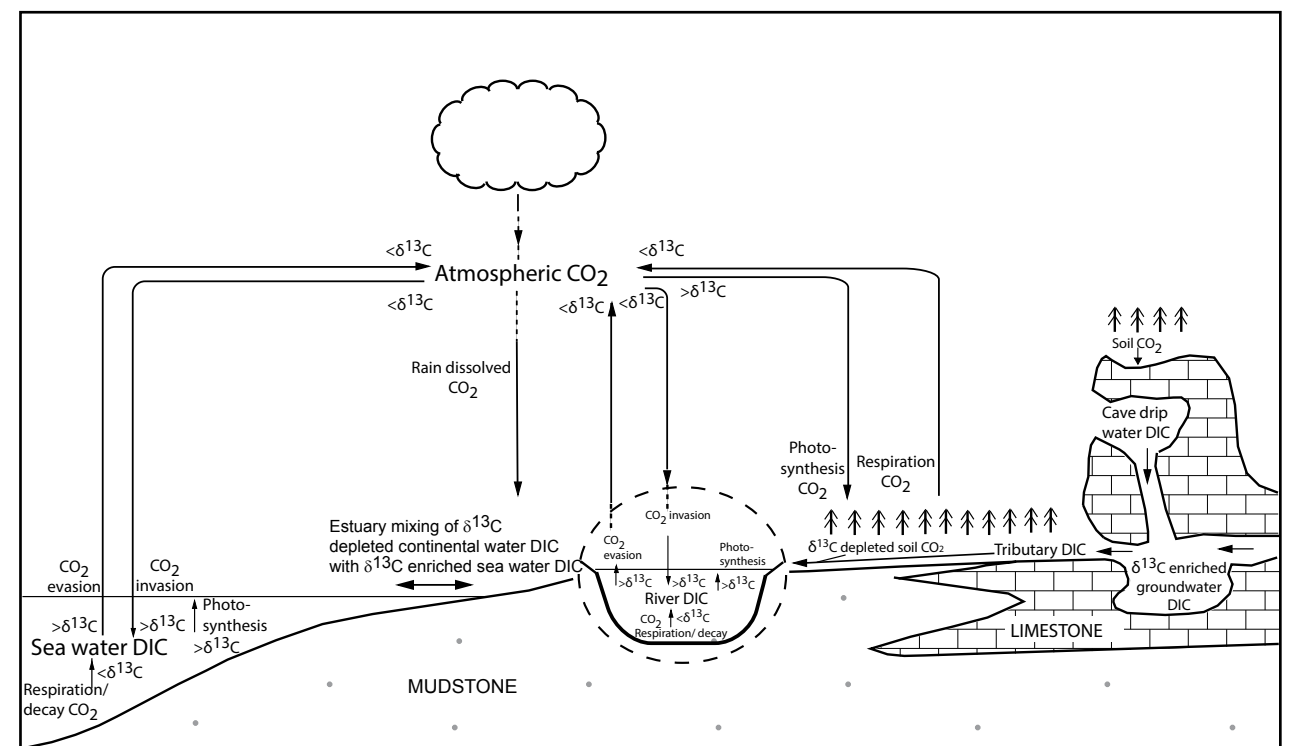


Figure 9.5. Schematic representation of $\delta^{13}\text{C}$ cycling in the Niah River watershed (riverine $\delta^{13}\text{C}$ DIC [dissolved inorganic carbon] systematics adapted from Atekwana & Krishnamurthy 1998).

composition (Atekwana & Krishnamurthy 1998). Some stream/river systems are dominated by groundwater recharge (Aravena & Suzuki 1990; Pawellek & Veizer 1994) and the isotopic signature of DIC will closely mirror that of the groundwater.

High biological activity, typical of tropical rainforest streams, promotes the addition of ^{13}C -depleted biogenic CO_2 (from soil and plant respiration and decay) and results in a decrease in the $\delta^{13}\text{C}$ DIC, whereas photosynthetic drawdown preferentially removes ^{12}C and enriches $\delta^{13}\text{C}$ DIC (Pawellek & Veizer 1994; Yang *et al.* 1996). Mixing with atmospheric CO_2 also enriches the $\delta^{13}\text{C}$ of the water body, with the lighter ^{12}C isotope preferentially degassed and the heavier ^{13}C isotope selectively exchanged from atmospheric CO_2 . Estuaries constitute an important source of CO_2 to the atmosphere and particularly so in tropical regions, with increased rates of oxidation and breakdown of organic matter creating large CO_2 overpressures and degassing (Longinelli & Edmond 1983; Quay *et al.* 1989; Richey *et al.* 2002). CO_2 evasion and subsequent $\delta^{13}\text{C}$ enrichment are therefore hypothesized to be of importance for the Sungai Niah. Residence time and equilibration of the water body with atmospheric CO_2 should also therefore be considered. The dissolution of Subis Limestone from reaction with acidic rainforest soils can also contribute to enriched $\delta^{13}\text{C}$ DIC at Niah, with values $\sim 0.4\text{‰}$ (Stephens 2004a).

Methods

Most of the shells in the Harrison Excavation Archive are kept in labelled bags which indicate the trench and spit-depth (e.g. E/A 0-6"). Taxa that occurred regularly (*Geloina erosa*, *Bellamyia javanica*, *Neritina zigzag* and *Paludomus* sp.) were sampled from successive depth intervals of the same excavation trenches, so that as much stratigraphic integrity as possible was maintained. *Neritina zigzag* is sometimes referred to in the literature as *N. ziczag*. The identification in this study of *Bellamyia javanica* was based on information in the Natural History Museum, London, and the study by Medway (1960a), but the detailed re-assessment of the material by Katherine Szabó after the completion of the isotope study reported in this chapter suggests that this snail is more likely to be *Cipangopaludina* cf. *chinensis* (this volume, Chapter 28). Hence in the rest of this chapter *Bellamyia javanica* is accompanied by an asterisk to mark its subsequent re-classification.

Initially shells were taken and analysed from bags labelled 'E/A' and 'E/G3' because of their relative abundance and the depths from which they had been collected in the Hell Trench. As described in Volume One, Chapter 2, the E/A and E/B series of trenches

were excavated in 1957 on either side of Trench E, the trench excavated in 1954. There is no 'Trench E/A' on the excavation plans, and a best guess is that this designation refers to trench E/A1, because a Harrison trench marker labelled E/A that appears to be *in situ* today is located where trench E/A1 is marked on the plans (Fig. 9.1). Also, E/A1 and E/G3 are close to the position of the Deep Skull, and because of the extensive removal of deposits from these locations by the original excavators, and the large area that the trenches cover, it is difficult to relate shells from E/A(1?) and E/G3 to the sedimentary layers or lithofacies identified by the NCP study (Volume One, Chapter 3; this volume, Chapter 5). Although the excavation of E/A probably removed sediments of Lithofacies 2C, 2 and 3, the E/A shells in the archive are most likely to derive from Lithofacies 2 or 2C rather than the archaeologically-sterile Lithofacies 3. E/G3 probably corresponds to Lithofacies 2C and possibly to the overlying Lithofacies 4.

The sampling was thereafter focused on a trench that could be related with greater confidence to the stratigraphy. Trench X/V1 at the back of the rock overhang was chosen since it had abundant shells and could be related to a position adjacent to deposits of Lithofacies 4 (Fig. 9.6). AMS radiocarbon dating of charcoal from the latter indicates deposition during the Late Pleistocene and Early Holocene (Volume One, Chapter 3; this volume, Chapter 5). Well-preserved specimens of *Bellamyia javanica** and *Geloina erosa* were taken from each sampling level of X/V1 where present (i.e. spit-depths 0-12", 12-24", 24-36" and 36-48"); none was found from spit 48-72"). The archive sample of shells was augmented by shells collected in the NCP 2000 excavations of Lithofacies 4 sediments under the rock overhang: ten well-preserved shells were taken from each context from contexts 1015-1017, and five from context 1018. All the shells selected for isotope analysis were put in labelled plastic bags, transported back to the UK, and stored in the cool store at Royal Holloway, University of London (RHUL). The organic periostracum was not preserved on any of the archaeological shell material.

Modern shells were sampled during the 2000, 2001 and 2002 field seasons (Fig. 9.7) with the following aims: (1) to find modern representatives of the shells found in the cave sediments to develop modern analogue calibration; (2) to understand isotopic variations within shells on a catchment scale; and (3) to make descriptions of their present macro- and micro-environments to aid isotopic calibration to known modern conditions (Table 9.1). Live molluscs were collected where possible to remove any uncertainty regarding their antiquity. Fresh-looking shells were

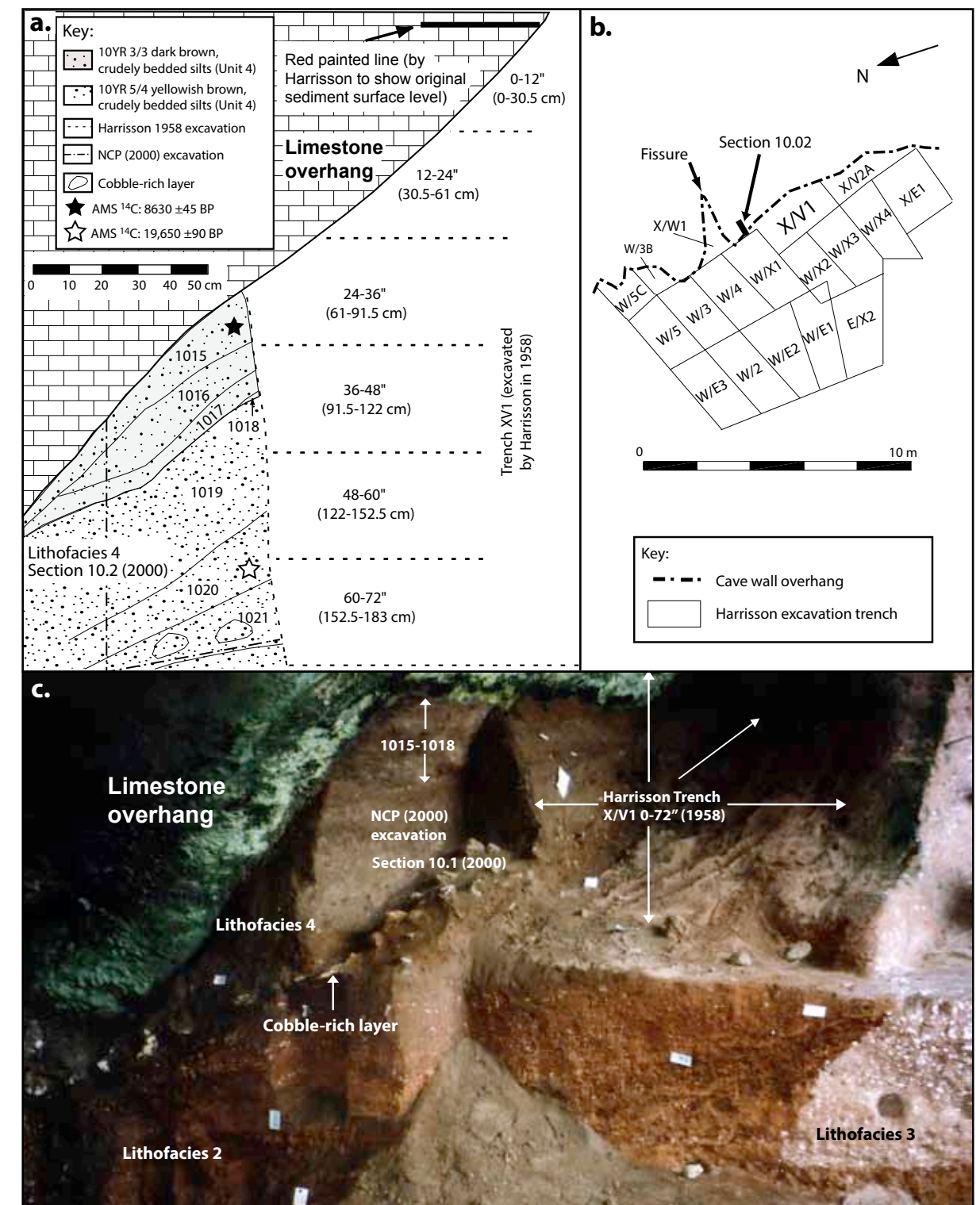


Figure 9.6. (a) Scale drawing looking 120° ESE at an exposure of Lithofacies 4 in Block B in Area A in the West Mouth (NCP Section 10.2(2000)), showing the likely relationship of the NCP contexts and Harrison Trench X/V1; (b) plan of the Harrison trenches in this part of the West Mouth; (c) looking southeast to the NCP excavation of Lithofacies 4 sediments in Block B under the rock overhang, showing the likely relationships of the NCP contexts and Harrison's Trench X/V1. (Photograph: M. Stephens.)

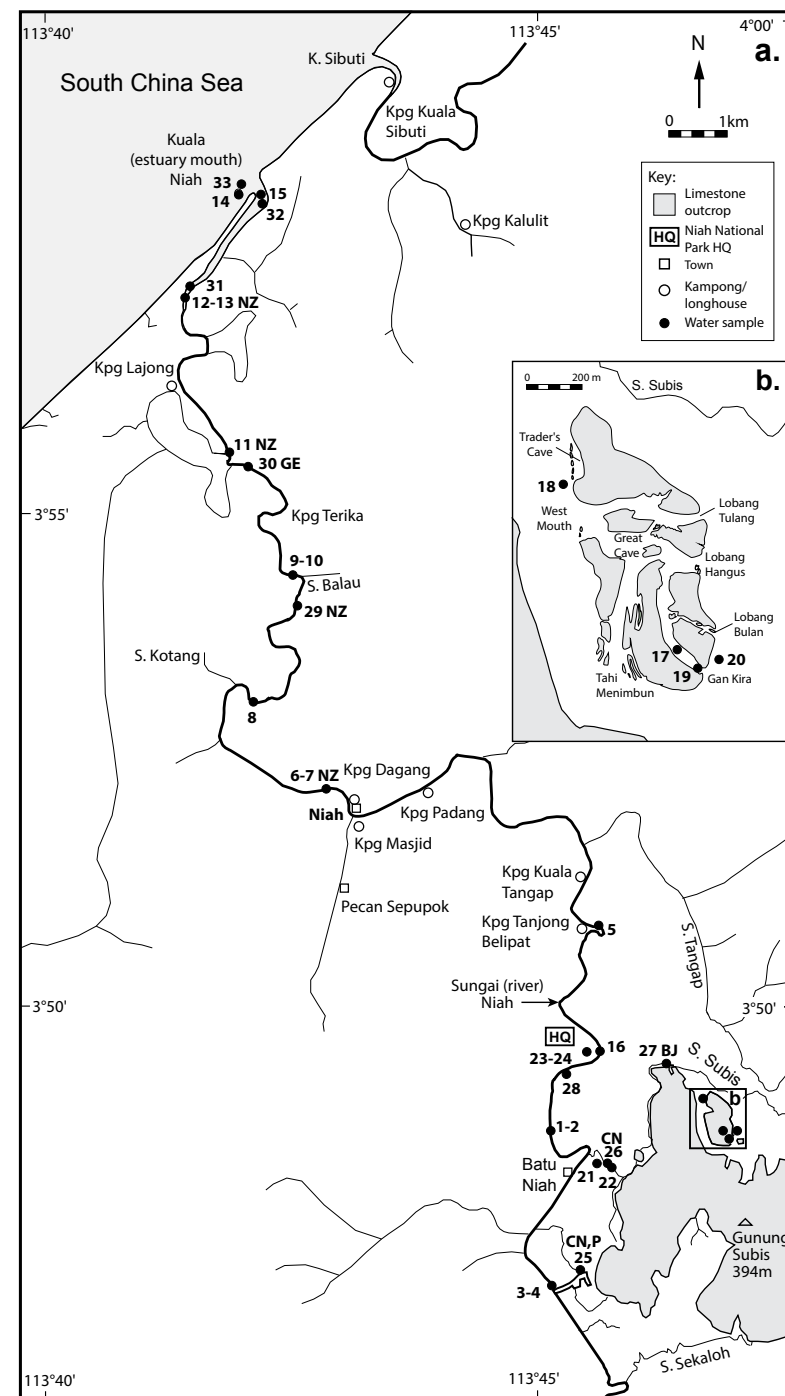


Figure 9.7. (a) Location of water samples collected in 2001 (1–22) and 2002 (23–33) from the Niah River catchment. Also indicated are the locations of molluscs in their natural habitat during the 2000–2002 field seasons, and subsequently analysed for stable isotopes (BJ: *Bellamya javanica**; CN: *Clea nigricans*; P: *Paludomus* sp.; GE: *Geloina erosa*; NZ: *Neritina zigzag*); (b) inset showing location of water samples collected around the Great Cave in 2001. S – Sungai (stream). The asterisk by *Bellamya javanica* denotes that, although this snail was identified as *Bellamya javanica* following Medway (1960a), the detailed re-assessment of the material by Katherine Szabó suggests that it is more likely to be *Cipangopaludina cf. chinensis*.

Table 9.1. Environmental information of modern mollusc shells analysed with stable isotopes in this study (listed in approximate order of proximity to the South China Sea). Where collection of live molluscs was possible, personal observations are included. All shells in this table are of aragonite mineralogy (Taylor et al. 1969, 1973; Dr. J. Taylor, pers. comm. 2004). See Stephens (2004a) for images of the modern shells analysed in this study. The asterisk by *Bellamya javanica* denotes that, although this snail was identified as *Bellamya javanica* following information in the Natural History Museum, London, and Medway (1960a), the detailed re-assessment of the material by Katherine Szabó suggests that this snail is more likely to be *Cipangopaludina cf. chinensis*.

Family	Genera/sp. and author	Habitat/environmental information	Live?
Ficidae	<i>Ficus</i> sp.	Sand dwellers in warm marine waters; subtidal marine predator.	No
Bursidae	<i>Bursa rana</i> (Linnaeus 1758)	Offshore marine; predator, eats ophiuroids and polychaetes. (Taylor 1980)	No
Cassidae	<i>Phalium</i> sp.	Marine predator, eats sea urchins and echinoids.	No
Xenophoridae	<i>Tugurium</i> sp.	Deep marine, algal suspension feeder.	No
Turritellidae	<i>Turritella terebra</i> (Linnaeus 1758)	Mostly subtidal marine sands but can be intertidal (e.g. Wong and Ahmad 1996); suspension feeder.	No
Carditidae	<i>Cardita</i> sp.	Shallow marine, attached to rocks.	No
Cultellidae	<i>Siliqua</i> sp.	Shallow marine; deep burrower of sandy beaches; deposit feeder.	No
Mactridae	<i>Mactra violacea</i> (Gmelin 1791)	Sandy mudflats in shallow water. (Wong & Ahmad 1996)	No
Veneridae	<i>Dosinia</i> sp.	Shallow marine water.	No
Arcidae	<i>Anadara cornea</i> (Reeve 1844)	Sandy beach and mudflats in shallow water. (Wong & Ahmad 1996)	No
Veneridae	<i>Meretrix meretrix</i> (Linnaeus 1758)	Shallow marine water but can be brackish; usually found buried in beaches; edible (Wong & Ahmad 1996)	No
Veneridae	<i>Marcia</i> sp.	Shallow marine water.	No
Melongenidae	<i>Volema myristica</i> (Röding 1798)	Shallow water in mud with fluctuating salinities; predator.	No
Arcidae	<i>Anadara granosa</i> (Linnaeus 1758)	Intertidal mudflats in front of mangroves; edible. (Richardson 1987)	No
Neritidae	<i>Neritina zigzag</i> (Lamarck 1816)	Found attached to estuarine mangrove plants e.g. Nipah palm (<i>Nypa fruticans</i>).	Yes
Corbiculidae	<i>Geloina erosa</i> (Solander 1786)	Found in substrate on landward side of mangroves with as little as 30% tidal coverage (Frith et al. 1976); occurring around streams draining through the mangal, feeding on suspended material in the water; utilises pedal gape to access groundwater during dry conditions (Morton 1976, 1984); breeds in summer (Morton 1985); edible.	Yes
Viviparidae	<i>Bellamya javanica</i> * (Von dem Busch 1844)	Found abundantly, submerged in upper reaches of freshwater Subis stream, but not towards the mouth, as also observed by Medway (1960: 377); feeds on algae.	Yes
Buccinidae	<i>Clea nigricans</i> (Adams 1855)	On bed of slow running freshwater Subis stream in lowland rainforest; predator, feeds on worms (oligochaetes).	Yes
Pleuroceridae	<i>Paludomus</i> sp.	On bed of slow running freshwater Subis stream in lowland rainforest.	Yes

collected where possible on the assumption that they had not been re-worked from much older sedimentary deposits. Except for *Bellamya javanica**, *Paludomus* sp., *Clea nigricans*, *Neritina zigzag* and *Geloina erosa*, all of the shells were found on the South China Sea beach, adjacent to the estuary of the Niah River (Kuala Niah). After collection, the mollusc shells were placed in labelled plastic bags. The live-collected molluscs were boiled in water and their soft parts then removed with tweezers.

To aid the calibration of the isotopic signatures in the modern shells to their surrounding environment, 125 ml water samples were collected from the same locations as the shell sampling points, in two successive years (23–27 April 2001; 11–22 April 2002), from seasonally wetter and drier periods, respectively (Fig. 9.8). For surface water samples the bottles were washed out twice in the water to be sampled, then held immersed till completely full. Bottom waters were sampled in April 2001, using a 5 litre *Patalas* water

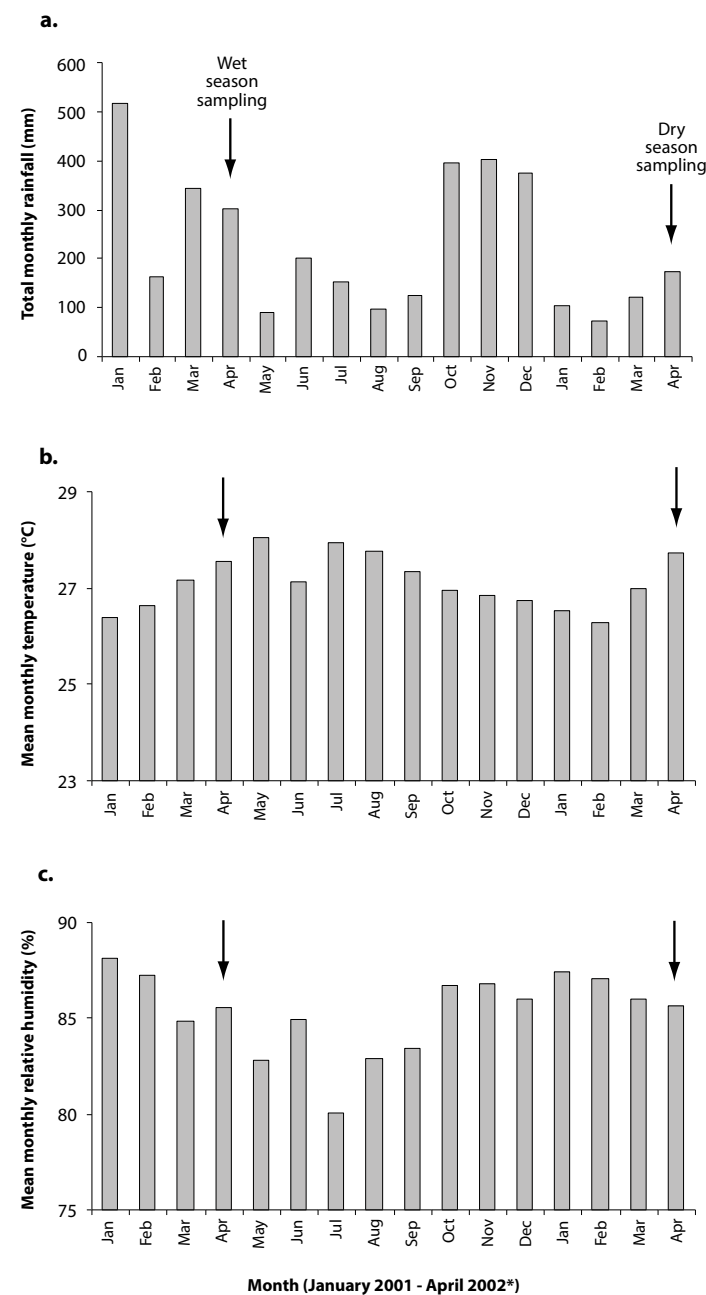


Figure 9.8. Water sampling periods at Niah (arrows) for stable isotopic analysis, in the context of meteorological parameters, January 2001 to April 2002*: (a) total monthly rainfall for Niah (Rangkaian Hidrologi Sarawak, Niah: 2001-2002 rainfall data); (b) mean monthly temperature for Miri (Malaysian Meteorological Service); (c) mean monthly relative humidity for Miri (Malaysian Meteorological Service). *April 2002 rainfall data were only recorded up until April 26th.

Table 9.2 Results of stable isotope analyses ($\delta^{13}\text{C}$ DIC, $\delta^{18}\text{O}$, $\delta^2\text{H}$) on replicate water samples from the Niah River basin. Results are given in δ notation, which reflects the % deviation from the international standards V-PDB (for water DIC - dissolved inorganic carbon) and V-SMOW (for oxygen and hydrogen isotopes of water).

Water sample no.	$\delta^{13}\text{C}$ VPDB (‰)		$\delta^{18}\text{O}$ VSMOW (‰)		$\delta^2\text{H}$ VSMOW (‰)	
	1st	2nd	1st	2nd	1st	2nd
1	-12.3	-	-8.0	-8.1	-50.2	-50.6
2	-	-	-8.0	-8.1	-51.0	-52.7
3	-11.7	-	-8.2	-8.2	-51.5	-51.1
4	-	-12.3	-8.2	-8.2	-51.9	-52.0
17	-7.3	-7.5	-6.7	-6.7	-38.5	-39.3
18	-13.8	-	-10.8	-10.7	-70.6	-71.3
19	-5.1	-5.9	-8.2	-8.2	-52.5	-54.0

sampler. The *Patalas* water sampler was lowered over the edge of the boat into the water, with the force of the water used to keep the hinged doors at the bottom and top of the sampler open. When the sampler was lowered to the required depth, the rope was pulled sharply upwards, closing the doors and terminating the flow of water into the sampler. The latter was then hauled to the surface and its contents poured into the sampling bottles via a rubber tube at the base of the sampler, making sure that the tube was inside the bottle to reduce the possibility of evaporation and exchange with the atmosphere, all of which could affect the isotopic composition. The bottles were sealed with PVC tape for the same reason. The water samples were transported back to the UK and stored in a cold store at RHUL. Replicates of water sample nos. 1, 2, 3, 4, 17, 18, 19 were taken for testing the reproducibility of isotopic results (Table 9.2).

The laboratory procedures are described in the Supplementary Material to this chapter.

Stable isotopic variations of waters in the Niah River catchment

The results of isotopic analyses ($\delta^{18}\text{O}$, $\delta^2\text{H}$ and $\delta^{13}\text{C}$ DIC) of the water from the Niah River catchment are set out in Table 9.3.

Flowing stream water of the Sungai Subis, sampled in the Niah National Park, displays the most depleted $\delta^{18}\text{O}$ (-8.4‰) and $\delta^2\text{H}$ (-54.7‰) values of the riverine samples (Fig. 9.9). The up-river to estuary surface waters range from -8.3‰ to -6.5‰ in $\delta^{18}\text{O}$, -52.7‰ to -41.6‰ in $\delta^2\text{H}$ in April 2001. Sea water, however, exhibits enriched values of $\delta^{18}\text{O}$ (-4.6‰) and $\delta^2\text{H}$ (-29.3‰) (Figs 9.9 and 9.10, Table 9.3). The Sungai Subis stream water sampled in 2002 exhibits similar $\delta^{18}\text{O}$

Table 9.3. Stable isotopic results of waters from the Niah River catchment, sampled between 23-27 April 2001 and 11-22 April 2002; see Figure 9.7 for sample locations. Additional information includes depth of water column sampled, air and surface water temperatures. For discussion of rain, cave drip, estuary mouth bottom water, rainforest pool and aquifer pool waters, see Stephens & Rose (2005). Results are given in δ notation, which reflects the % deviation from the international standards V-PDB (for water DIC - dissolved inorganic carbon) and V-SMOW (for oxygen and hydrogen isotopes of water).

No.	Sample point description	Sample date	Depth below surface (m)	$\delta^{13}\text{C}$ VPDB (‰)	$\delta^{18}\text{O}$ VSMOW (‰)	$\delta^2\text{H}$ VSMOW (‰)
1	Niah River	26.04.01	1.0	-12.3	-8.0	-50.2
1R	Niah River	26.04.01	1.0		-8.1	-50.6
2	Niah River	26.04.01			-8.0	-51.0
2R	Niah River	26.04.01			-8.1	-52.7
3	Niah River	26.04.01	0.8	-11.7	-8.2	-51.5
3R	Niah River	26.04.01	0.8		-8.2	-51.1
4	Niah River	26.04.01			-8.2	-51.9
4R	Niah River	26.04.01		-12.3	-8.2	-52.0
5	Niah River	26.04.01			-7.9	-50.6
6	Niah River	26.04.01		-11.6	-7.7	-43.5
7	Niah River	26.04.01	9.0		-7.7	-49.9
8	Niah River	26.04.01	0.9	-11.5	-7.6	-48.0
9	Niah River	26.04.01	1.2	-11.6	-7.5	-47.0
10	Niah River	26.04.01	8.0	-10.8	-7.5	-36.8
11	Niah River	26.04.01		-10.7	-7.5	-48.0
12	Niah River	26.04.01		-11.0	-7.1	-46.4
13	Niah River	26.04.01	5.0	-1.7	-1.5	-11.1
14	South China Sea	26.04.01		-4.8	-4.6	-29.3
15	Niah River estuary	26.04.01		-8.1	-6.5	-41.6
16	Niah River	27.04.01			-8.3	-52.4
17	Gan Kira interior drip	23.04.01		-7.3	-6.7	-38.5
17R	Gan Kira interior drip	23.04.01		-7.5	-6.7	-39.3
18	Rain	25.04.01		-13.8	-10.8	-70.6
18R	Rain	25.04.01			-10.7	-71.3
19	Gan Kira mouth drip	23.04.01		-5.1	-8.2	-52.5
19R	Gan Kira mouth drip	23.04.01		-5.9	-8.2	-54.0
20	Rain	23.04.01			-4.8	-26.0
21	Rainforest pool	27.04.01		-14.6	-7.3	-44.6
22	Subis Stream	27.04.01		-14.5	-8.4	-54.7
23	Rain	14.04.02			-2.2	-9.1
24	Rain	17.04.02			-3.6	-12.0
25	Aquifer pool	21.04.02			-8.3	-52.8
26	Subis Stream	21.04.02			-8.0	-48.2
27	Subis Stream	11.04.02			-6.1	-35.9
28	Niah River	22.04.02			-4.6	-19.8
29	Niah River	22.04.02			-5.3	-30.6
30	Niah River	22.04.02			-5.1	-28.9
31	Niah River estuary	22.04.02			-4.0	-21.7
32	Niah River estuary	22.04.02			-3.7	-20.5
33	South China Sea	22.04.02			-0.3	-2.9

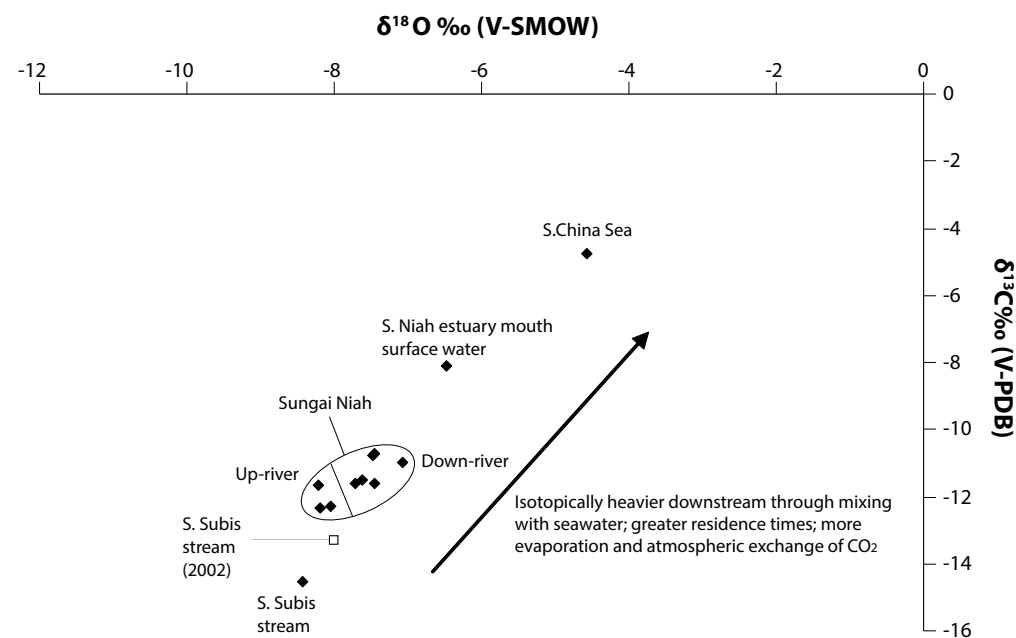


Figure 9.9. Plot of $\delta^{18}\text{O}$ vs. $\delta^{13}\text{C}$ for water samples from the Niah River catchment. April 2001 data are represented as diamonds and the April 2002 data-point is represented by an open square.

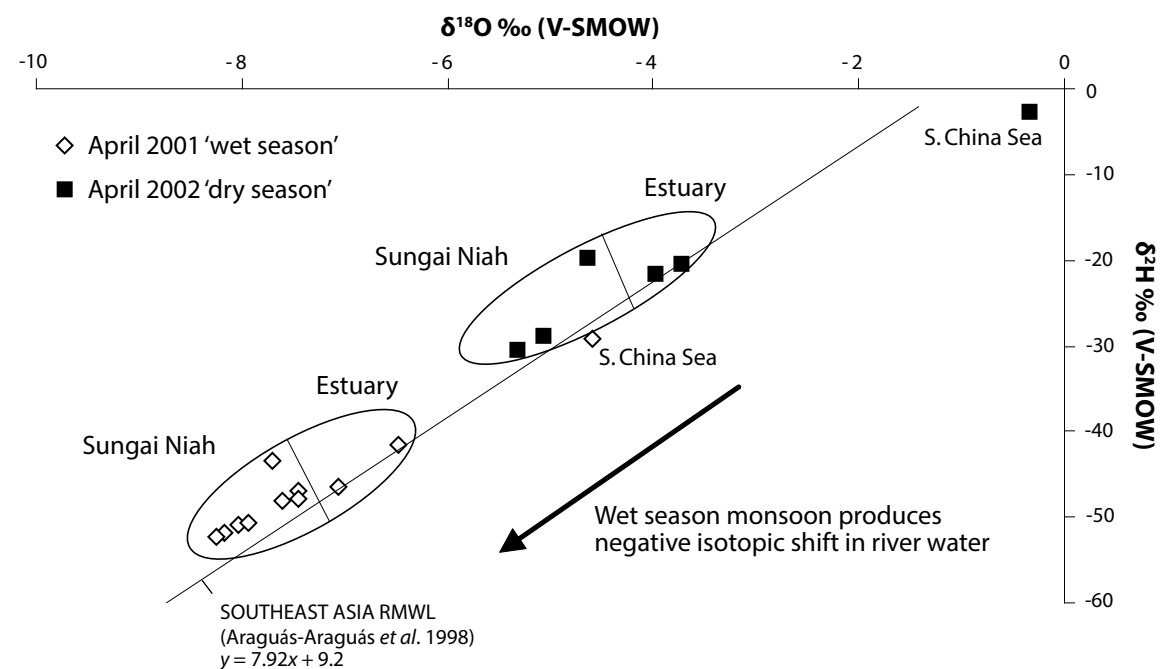


Figure 9.10. Plot of $\delta^{18}\text{O}$ vs. $\delta^2\text{H}$ for Niah River waters collected in the wet period of April 2001 and the dry period of April 2002. Both data-sets are placed in the context of the Southeast Asia Regional Meteoric Water Line (RMWL) collated by Araguás-Araguás et al. (1998).

(-8‰) to that sampled in 2001 (Fig. 9.9). In comparison to 2001, the Sungai Niah waters of 2002 are relatively heavier by ~2‰ (Fig. 9.10). As also found from the 2001 waters, the 2002 Niah estuary (Kuala Niah) waters are heavier than their downriver counterparts in $\delta^{18}\text{O}$ and $\delta^2\text{H}$, by ~1‰ and ~10‰, respectively (Fig. 9.10). The April 2002 South China Sea water exhibits the most enriched $\delta^{18}\text{O}$ (-0.3‰) and $\delta^2\text{H}$ (-2.9‰) values of all the water samples (Fig. 9.10). All water samples plot on or close to the Southeast Asia RMWL.

The tributary rainforest stream (Sungai Subis) exhibits the lightest isotopic values compared with those of the estuary and sea, which get progressively heavier. This is typical of tributaries that have less residence time than the main river (Yang *et al.* 1996) and so undergo less evaporation, which is further enhanced by tree canopy shade. The progressive enrichment of waters towards the sea is due to increased evaporation and the natural widening and reduction in speed of the estuary, creating a larger surface area, longer residence time, and a reduced air temperature necessary for evaporation. Also particularly important in the estuary zone is mixing with enriched evaporated saline sea waters. The significantly lighter $\delta^{18}\text{O}$ and $\delta^2\text{H}$ values of the 2001 Niah River samples, in comparison with those of 2002, are most likely due to the 'amount effect' through the heavier rainfall during and preceding April 2001 (Fig. 9.8). The similarity in isotopic values for the Sungai Subis stream in the wetter April 2001 and drier April 2002 could indicate the importance of groundwater recharge. Niah waters plot on or close to the Southeast Asia RMWL, indicating that they are in equilibrium with, and therefore a good indicator of, regional climatic processes (also see Cobb *et al.* 2007).

The 2001 and 2002 samples from the flowing rainforest stream display the most depleted $\delta^{13}\text{C}$ riverine values, with the 2001 sample being slightly lighter in $\delta^{13}\text{C}$ (-14.5‰ and -13.3‰, respectively). The up-river to estuary mouth surface waters are more enriched and range from -12.3‰ to -8.1‰ and sea water enriched further still (-4.8‰) (Fig. 9.9; Table 9.3). Investigations of $\delta^{13}\text{C}$ variations in several estuaries indicate that dissolution of carbonate minerals ($\delta^{13}\text{C} = \sim 0\text{‰}$) with biogenic carbon ($\delta^{13}\text{C} = -25\text{‰}$) in the soil zone usually produces an intermediate $\delta^{13}\text{C}$ value of ~-12‰ (Craig 1953; Spiker 1980) unless there is limited carbonate weathering in the basin, when water $\delta^{13}\text{C}$ values are typically ~-20‰ (Longinelli & Edmond 1983). The arctic Mackenzie drainage basin, however, has reduced biological activity and, in addition, a strong influence of carbonate dissolution producing enriched values of ~-9‰ (Hitchon & Krouse 1972). Thus in a basin such as that of the Niah River, where

there is high biological activity and limestone bedrock, values more negative than -12‰ can be attributed to additional biogenic CO_2 , with more positive values reflecting a greater importance of photosynthetic activity and atmospheric exchange.

The lightest $\delta^{13}\text{C}$ values in the Niah basin occur for the tributary stream (~-14‰), reflecting the dominant influence of biogenic respiration and decay. This contrasts with the main river that has no canopy shade and greater surface area for photosynthetic and atmospheric exchange. Up-river values have more enriched $\delta^{13}\text{C}$ values of ~-12‰ and become slightly more enriched towards the sea, reflecting mixing with enriched sea water, increased photosynthetic activity associated with a reduction in turbidity (personal observation, April 2002) and increased residence time as the estuary widens and atmospheric CO_2 exchange becomes more important. The slightly lighter Sungai Subis stream water $\delta^{13}\text{C}$ of April 2001, in comparison with that of 2002, could be related to the greater rainfall of 2001 and the possible increased inwash of isotopically-light biogenic carbon from lowland soils.

In both the April 2001 and April 2002 sampling periods a progressive isotopic enrichment generally occurs towards the South China Sea from the lowland rainforest drainage through to the estuary. Comparison of the 2001 and 2002 data reveals significantly lighter $\delta^{18}\text{O}$ and $\delta^2\text{H}$ in the Niah River waters of April 2001, most likely as a result of the heavier rainfall of that period and the 'amount effect'. Modern geographic trends can thus be evaluated from the Niah hydrology data (also see Cobb *et al.* 2007), confirming the potential for the calibration of the Late Quaternary stable isotope proxy data preserved in the deposits of the West Mouth (Stephens & Rose 2005).

Stable isotope analyses of modern shells from the Niah River catchment

Figure 9.11 presents a $\delta^{18}\text{O}$ vs. $\delta^{13}\text{C}$ bi-plot of mean and standard deviation values from growth profile sampling of modern shells from varying aquatic habitats in the Niah catchment (Table 9.1). These habitats range from offshore marine (*Ficus* sp., *Bursa rana*, *Phalium* sp., *Tugurium* sp., *Turritella terebra* and *Cardita* sp.) with a mean $\delta^{18}\text{O}$ range of -3‰ to -3.9‰; $\delta^{13}\text{C}$ 2‰ to -0.5‰, to shallower water, intertidal mudflat dwellers (*Siliqua* sp., *Macra violacea*, *Dosinia* sp., *Anadara cornea*, *Meretrix meretrix*, *Marcia* sp. and *Volema myristica*) with a mean $\delta^{18}\text{O}$ range of -5‰ to -3.5‰; $\delta^{13}\text{C}$ -1‰ to -7.5‰, to more brackish water estuarine species (*Anadara granosa*, *Geloina erosa* and *Neritina zigzag*) with a mean $\delta^{18}\text{O}$ range of -6.5‰ to -9‰; $\delta^{13}\text{C}$ -6.4‰ to -13.6‰, to the freshwater stream

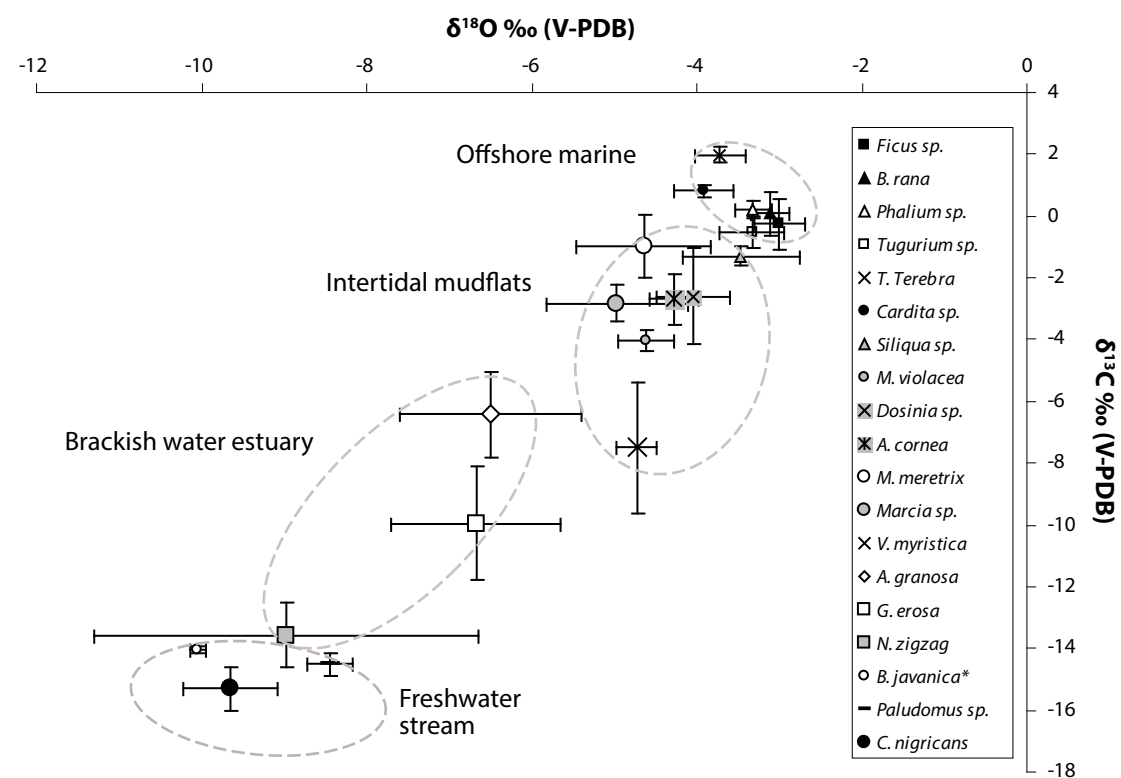


Figure 9.11. $\delta^{18}\text{O}$ vs. $\delta^{13}\text{C}$ from growth profile analyses of individual modern shells from varying sub-environments of the Niah River catchment. The asterisk by *Bellamyia javanica* denotes that, although this snail was identified as *Bellamyia javanica* from information in the Natural History Museum, London, and following Medway (1960a), the detailed re-assessment of the material by Katherine Szabó suggests that it is more likely to be *Cipangopaludina cf. chinensis*.

molluscs *Bellamyia javanica**, *Paludomus* sp. and *Clea nigricans* with a mean $\delta^{18}\text{O}$ range of -8.4‰ to -10‰ $\delta^{18}\text{O}$; $\delta^{13}\text{C}$ -14‰ to -15.3‰). Of the Niah shells studied, the offshore marine and freshwater shells exhibit the smallest stable isotopic variation: mean $\delta^{18}\text{O}$ standard deviation 0.3‰ ; mean $\delta^{13}\text{C}$ standard deviation 0.5‰ and 0.4‰ , respectively. The intertidal shells exhibit intermediate values (mean $\delta^{18}\text{O}$ st. dev. 0.5‰ ; mean $\delta^{13}\text{C}$ st. dev. 1‰). The estuarine shells show the greatest stable isotopic variation (mean $\delta^{18}\text{O}$ standard deviation 1.5‰ ; mean $\delta^{13}\text{C}$ st. dev. 1.4‰).

These results, the first ever isotopic studies of the taxa involved, indicate that isotopic signals can be used to separate the shells into environmental sub-groups according to habitat: the marine shells exhibit enriched values typical of more evaporated and saline seawater; the estuarine shells exhibit a median value, and a wider range of values, as a result of the mixing of freshwater and seawater; the freshwater shells have very depleted values typical of a stream environment in rainforest with less evaporation and high biological

activity (Keith *et al.* 1964). It even appears that the mollusc shells have an isotopic signal that is representative of their particular micro-habitat. For example, *Anadara granosa* and *Geloina erosa* are both classified as living in the estuarine zone, but *Geloina erosa* is typically found on the landward side of mangroves with less tidal coverage and so greater freshwater influence (Frith *et al.* 1976; Table 9.1), and it exhibits lighter stable isotopic values.

The small stable isotopic variation of marine shells is likely to be due to the stability of the marine habitat away from the influence of river inputs (Aguirre *et al.* 1998), whereas intertidal shells will be more susceptible to significant freshwater runoff events and hence greater isotopic variation. Smaller stable isotopic variation in the shells of molluscs that inhabit freshwater streams is also probably due to a less dynamic environment, with no mixing of isotopically-enriched saline waters. The freshwater shell isotope profile is likely to be sensitive to the factors governing recharge of the stream environment, i.e. rainfall and

groundwater. Seasonal changes in monsoon rainfall do not appear to be recorded in the freshwater shells, possibly due to the homogenisation of the monsoon signal through groundwater mixing. The age of groundwaters at Niah is unknown, but given the wet tropical climate of Sarawak it is possible that they are recycled in tens of years rather than the hundreds or thousands of years as is the case, for example, in the UK. As a result, whole shell analyses of freshwater shells from Niah may be suitable to provide informa-

tion on the isotopic signal of groundwater (ultimately fed by rainwater), with implications for variability in meteorological circulation patterns and climate change.

The two modern specimens of *Geloina erosa* exhibit 'saw-tooth' stable isotopic profiles, with broad co-variation between $\delta^{18}\text{O}$ and $\delta^{13}\text{C}$ for each modern shell (Fig. 9.12). Both modern shells also have similar mean $\delta^{18}\text{O}$ (MOG1: -6.7‰ ; MOG2: -6.4‰) and $\delta^{13}\text{C}$ values (MOG1: -9.9‰ ; MOG2: -9.5‰), respectively. Peaks (negative shifts of $\delta^{13}\text{C}$ and $\delta^{18}\text{O}$) in the sta-

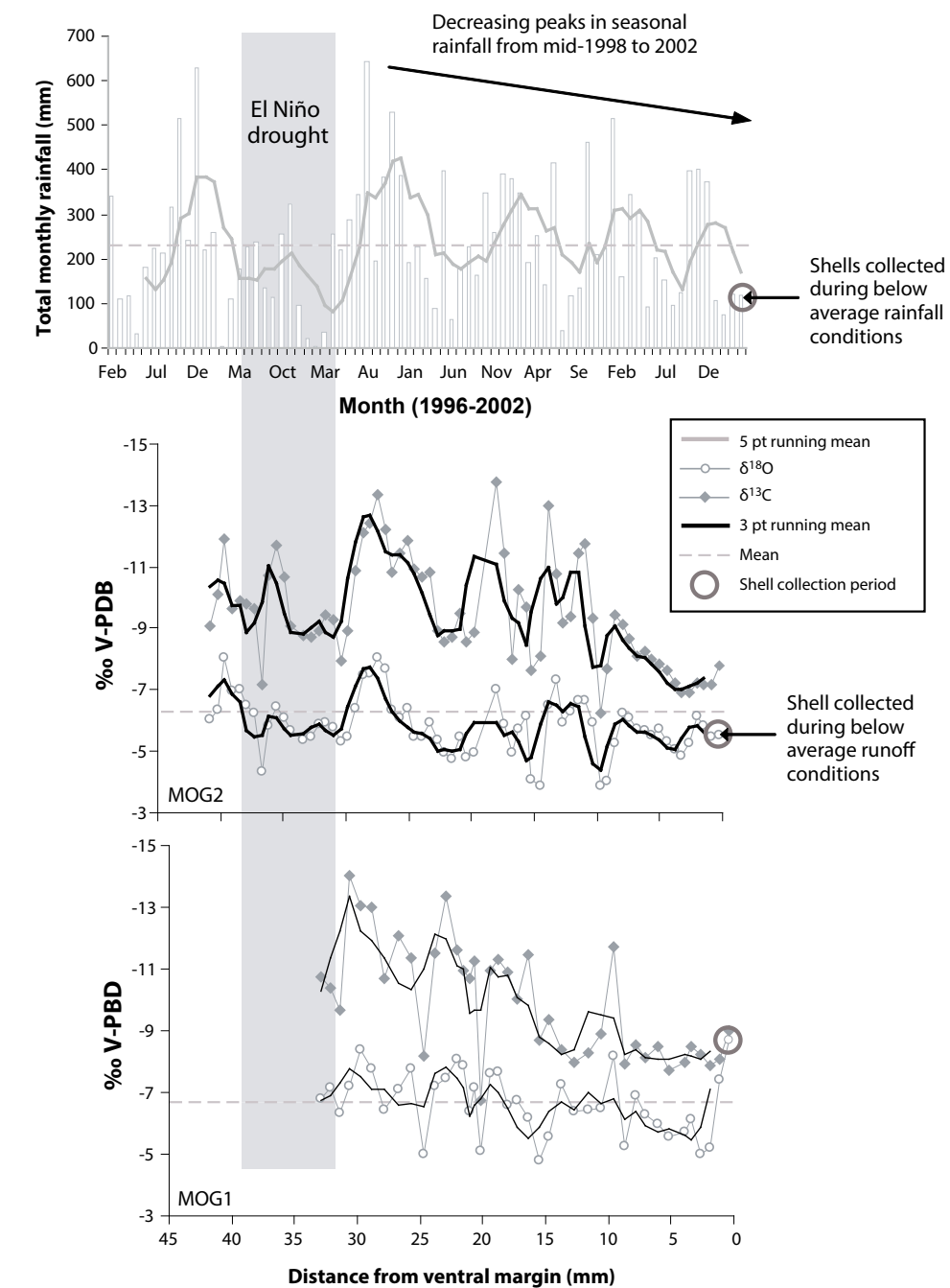


Figure 9.12. Comparison of (upper) modern rainfall for Niah with (mid and lower) modern isotopic profiles of two modern *Geloina erosa* shells. Note the 1997–1998 El Niño drought marker horizon. A five point running mean trendline is used for the rainfall data, in comparison with a three point running mean trendline used for the isotopic data. Open circle symbols represent $\delta^{18}\text{O}$ and filled diamond symbols represent $\delta^{13}\text{C}$. A reversed isotopic scale is used with which to compare the peaks and troughs of rainfall. Rainfall peaks around the northeast monsoon (typically November to March) and reduced rainfall occurs during the southwest monsoon (typically June to September).

ble isotopic profiles of both modern shells exhibit a general decreasing trend (i.e. become isotopically heavier) towards the ventral margin. The seasonal peaks of rainfall associated with the northeast (winter) monsoon at Niah from mid-1998 to 2002 also exhibit a similar decreasing trend (Fig. 9.12, upper). From March 1997 to March 1998, however, relatively very little rain fell at Niah. A similar trough (isotopic enrichment) occurs between 35 and 30 mm in the stable isotopic profile of MOG2 (Fig. 9.12, mid). The $\delta^{18}\text{O}$ value of the last growth increment of MOG2 (-5.5‰) is more positive than the mean $\delta^{18}\text{O}$ value for the shell profile of MOG2 (-6.4‰). The $\delta^{18}\text{O}$ value of the last growth increment of MOG1 (-8.7‰), however, is more negative than the mean $\delta^{18}\text{O}$ value for the shell profile of MOG1 (-6.7‰).

The broad co-variation between $\delta^{18}\text{O}$ and $\delta^{13}\text{C}$ in each modern shell implies a common forcing factor controlling the seasonal fractionations of oxygen and carbon isotopes in the estuary, such as the heavy northeast monsoon rains of November to March in Sarawak. Negative shifts in $\delta^{18}\text{O}$ are typical of heavy monsoon rains associated with the gradual rainout of moist air masses moving inland forced by monsoon circulation (Araguás-Araguás *et al.* 1998; Dansgaard 1964). The subsequent flooding reduces seawater influence and salinity and produces negative $\delta^{13}\text{C}$ DIC values in the estuary (Stephens & Rose 2005). In addition, negative $\delta^{13}\text{C}$ peaks in these shells may be the result of increased metabolic CO_2 derived from feeding (e.g. Vander Putten *et al.* 2000) associated with the runoff of nutrients and soil particles (Kazungu *et al.* 1989). *Geloina erosa* does not, however, appear to use metabolically-derived CO_2 to build its shell during summer months when reproductive activity occurs (Morton 1985), as negative shifts in $\delta^{13}\text{C}$ would also occur in this period.

This isotopic pattern has been observed for other estuarine molluscs and also attributed to seasonal mixing of freshwater and seawater in the estuary with the negative isotopic shifts related to pulses of freshwater (Khim *et al.* 2003; Leng & Pearce 1999; Tripathi *et al.* 2001). The decreasing trend in the peaks of the stable isotopic profiles might reflect decreasing runoff. This inference is supported by the similar decreasing trend of seasonal rainfall recorded at Niah from mid 1988 to 2002 (Fig. 9.12, upper). Previous studies of *Geloina erosa* suggest a lifespan of around four years (Clemente & Ingole 2011) and this would broadly fit with the suggested correlation of the isotope profiles with the rainfall data (Fig. 9.12). The low rainfall at Niah from March 1997 to March 1998 was in response to the El Niño event that caused prolonged dry conditions in Sarawak (Nakagawa *et al.* 2000). The similar isotopic

enrichment trough in MOG1 may thus be a marker of the El Niño drought.

The higher than average $\delta^{18}\text{O}$ value for the last growth increment of MOG2 (Fig. 9.12, mid) is what would be expected since it was collected during a period of low rainfall. This indicates that $\delta^{18}\text{O}$ analysis of the last growth increments of shell profiles of *Geloina erosa* has the potential to reveal information on the timing of collection in prehistoric times at Niah. On the other hand, the last growth increment of MOG1 displays a lower than average $\delta^{18}\text{O}$ value (Fig. 9.12, lower), incorrectly indicating that this shell was collected during a period of higher than usual rainfall/runoff. The analysis of further modern shells is required to resolve this discrepancy.

Stable isotopic analyses of shells from archaeological deposits in the West Mouth

All of the archaeological shells have lighter ranges of $\delta^{18}\text{O}$ than those found in their modern counterparts. For $\delta^{13}\text{C}$, however, only the estuarine mollusc shells *Geloina erosa* from Trenches X/V1 (Fig. 9.13) and E/G3 (Fig. 9.14) and *Neritina zigzag* from Trench E/A(?) (Fig. 9.15) exhibit generally lighter mean ranges than those found in their modern equivalents. Shells of *Geloina erosa* from X/V1 have $\delta^{13}\text{C}$ values that lie between -13.7 to -10.2‰ and those from E/G3 have $\delta^{13}\text{C}$ values that lie between -14.2 to -9.5‰ compared with their modern equivalents that lie between -11.7 to -7.8‰. Shells of *Neritina zigzag* from E/A have $\delta^{13}\text{C}$ values that lie between -13.5 to -11.3‰ compared with their modern equivalents that lie between -13.3 to -10.1‰. Conversely, the prehistoric freshwater shells *Bellamyia javanica** from X/V1 (Fig. 9.16) and NCP (Fig. 9.17) and *Paludomus* sp. from E/A (Fig. 9.18) exhibit heavier mean ranges in $\delta^{13}\text{C}$ than those found in their modern equivalents. Shells of *Bellamyia javanica** from X/V1 have $\delta^{13}\text{C}$ values that lie between -13.9 to -11.9‰ and those from the NCP excavations have $\delta^{13}\text{C}$ values that lie between -13.4 to -11‰ compared with their modern equivalents that lie between -14.1 to -12.9‰. Shells of *Paludomus* sp. from E/A have $\delta^{13}\text{C}$ values that lie between -13.7 to -10.1‰ compared with their modern equivalents that lie between -14.9 to -14.8‰.

Prehistoric shells of *Geloina erosa* from both X/V1 (Fig. 9.13) and E/G3 (Fig. 9.14) exhibit significantly smaller ranges in $\delta^{13}\text{C}$ than those found in modern specimens, whereas similar ranges in $\delta^{18}\text{O}$ exist between the prehistoric and modern shells. Prehistoric shells of *Neritina zigzag* also show smaller ranges in $\delta^{13}\text{C}$ than in their modern counterparts (Fig. 9.15). Prehistoric shells of *Bellamyia javanica** from X/V1 (Fig. 9.16) and NCP (Fig. 9.17), conversely, exhibit smaller

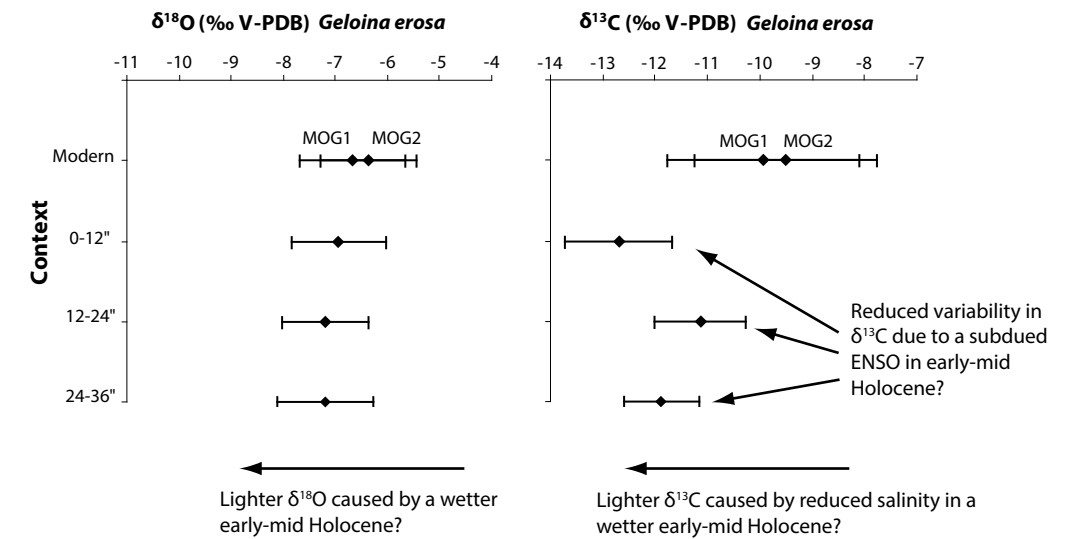


Figure 9.13. Mean and standard deviation of the $\delta^{18}\text{O}$ and $\delta^{13}\text{C}$ profiles from laser ablation analyses of *Geloina erosa* from successive spit-depths of Trench X/V1 (samples from the Harrison Excavation Archive). Analyses of the two modern *Geloina erosa* shells following laser ablation analysis are shown for comparison. Note: 12" (inches) = 30.5 cm.

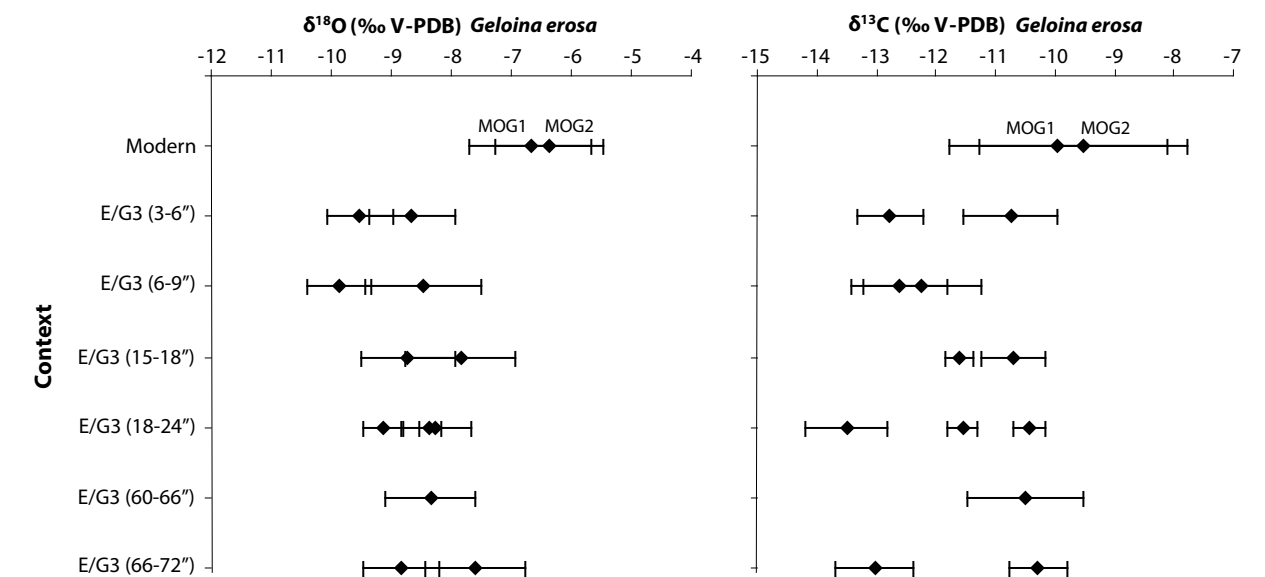


Figure 9.14. Mean and standard deviation of $\delta^{18}\text{O}$ and $\delta^{13}\text{C}$ profiles from growth profile drilling of individual *Geloina erosa* shells from successive spit-depths of Trench E/G3 (samples from the Harrison Excavation Archive). Mean and standard deviation of two modern *Geloina erosa* shells following laser ablation analysis are shown for comparison. Note, 1" (inch) = 2.54 cm.

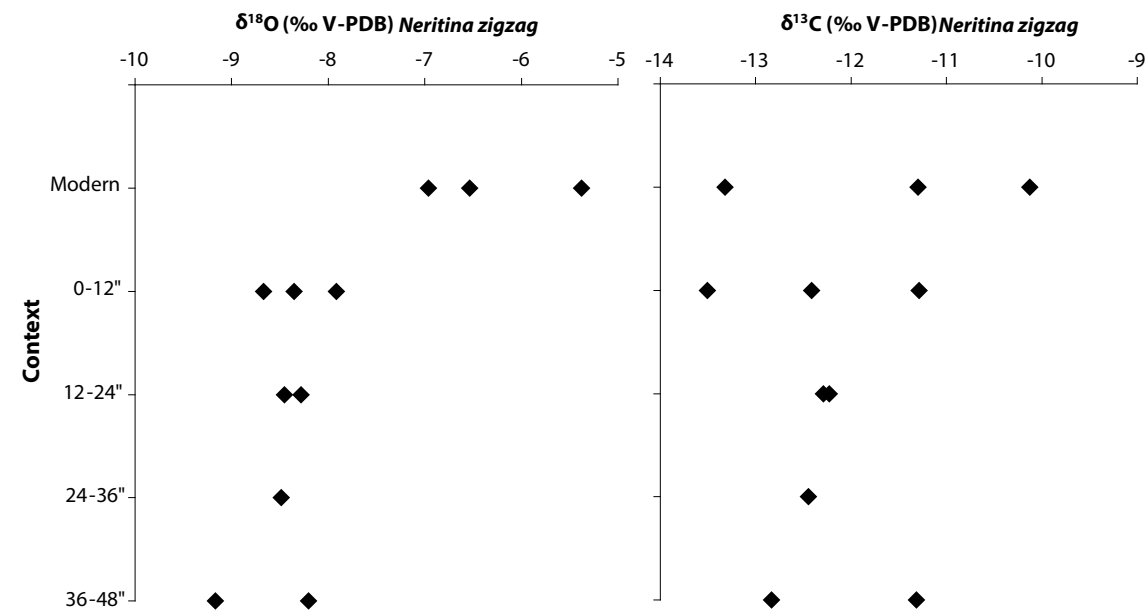


Figure 9.15. $\delta^{18}\text{O}$ and $\delta^{13}\text{C}$ of half-shell analyses of *Neritina zigzag* from successive spit-depths of Trench E/A (samples from the Harrison Excavation Archive). Half-shell analyses of three modern *Neritina zigzag* shells (collected live in 2001) are shown for comparison.

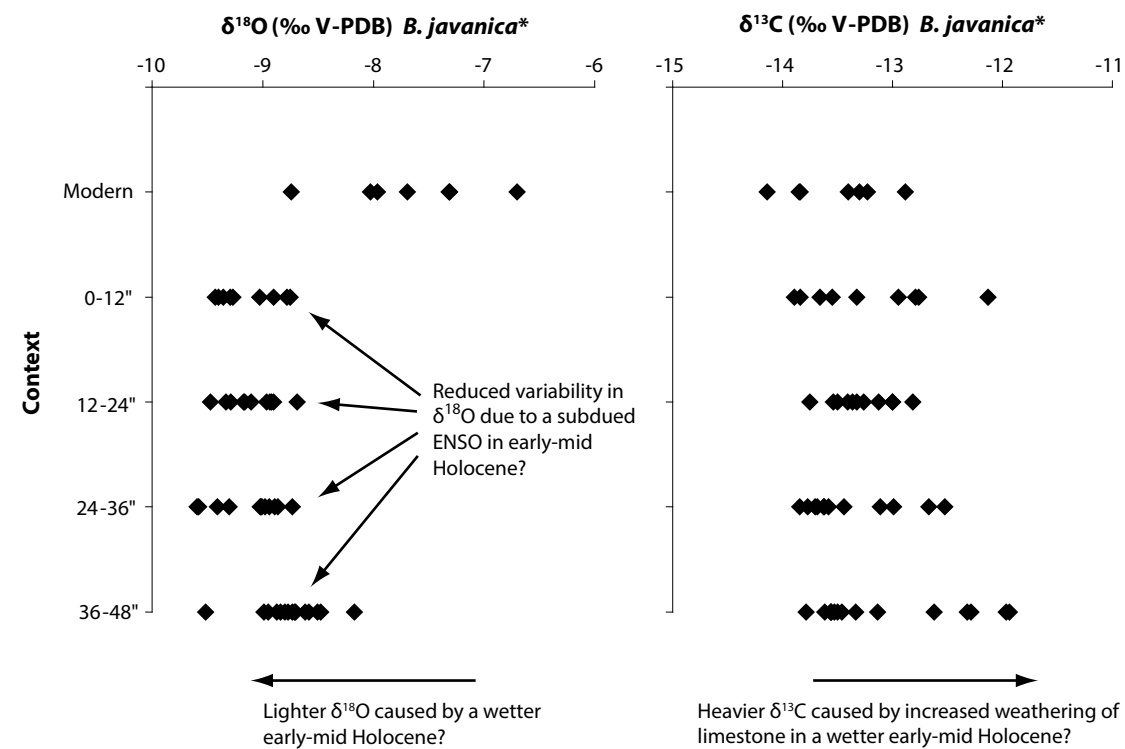


Figure 9.16. $\delta^{18}\text{O}$ and $\delta^{13}\text{C}$ of whole-shell analyses of *Bellamya javanica** from successive spit-depths of Trench XI/V1 (samples from the Harrison Excavation Archive). Analyses of six modern *Bellamya javanica** shells are shown for comparison. Note: 12" = 30.5 cm. The asterisk by *Bellamya javanica* denotes that, although this snail was identified as *Bellamya javanica* following information in the Natural History Museum, London, and Medway (1960a), the detailed re-assessment of the material by Katherine Szabó suggests that it is more likely to be *Cipangopaludina cf. chinensis*.

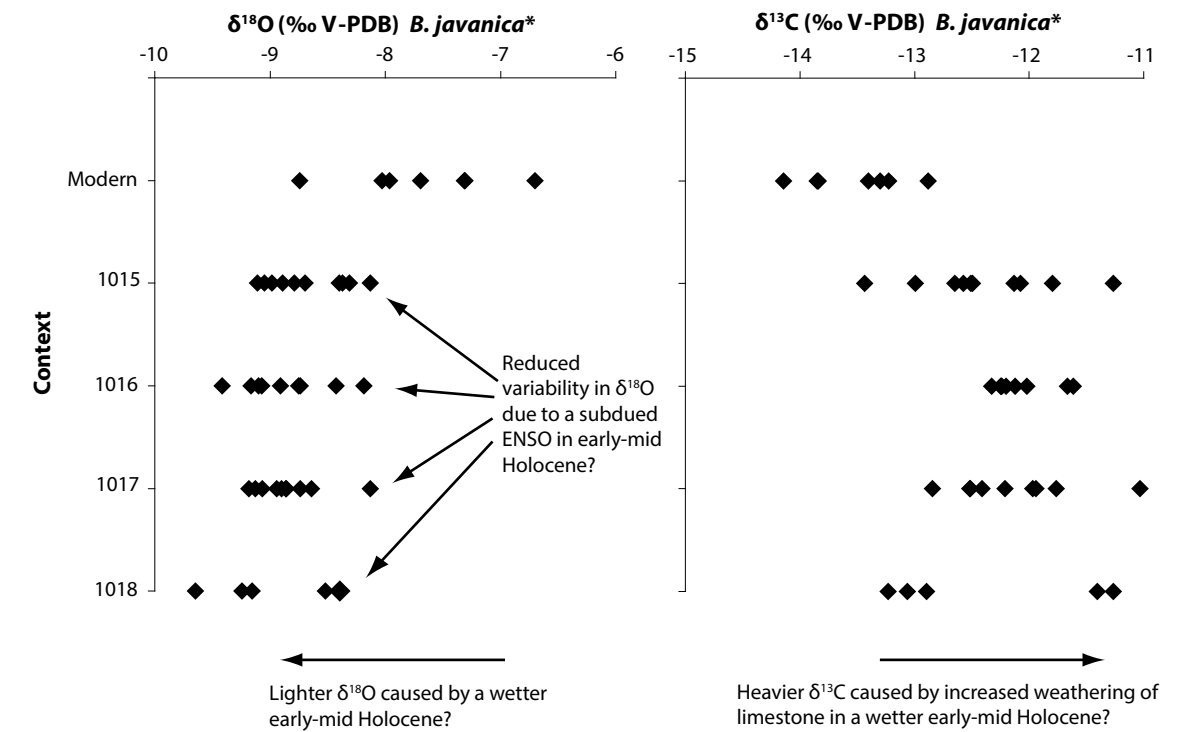


Figure 9.17. $\delta^{18}\text{O}$ and $\delta^{13}\text{C}$ of whole-shell analyses of *Bellamya javanica** from NCP excavation contexts 1015-1018 (see Figure 9.6a). Modern *Bellamya javanica** results are also plotted for comparison. The asterisk by *Bellamya javanica* denotes that, although this snail was identified as *Bellamya javanica* following information in the Natural History Museum, London, and Medway (1960a), the detailed re-assessment of the material by Katherine Szabó suggests that it is more likely to be *Cipangopaludina cf. chinensis*.

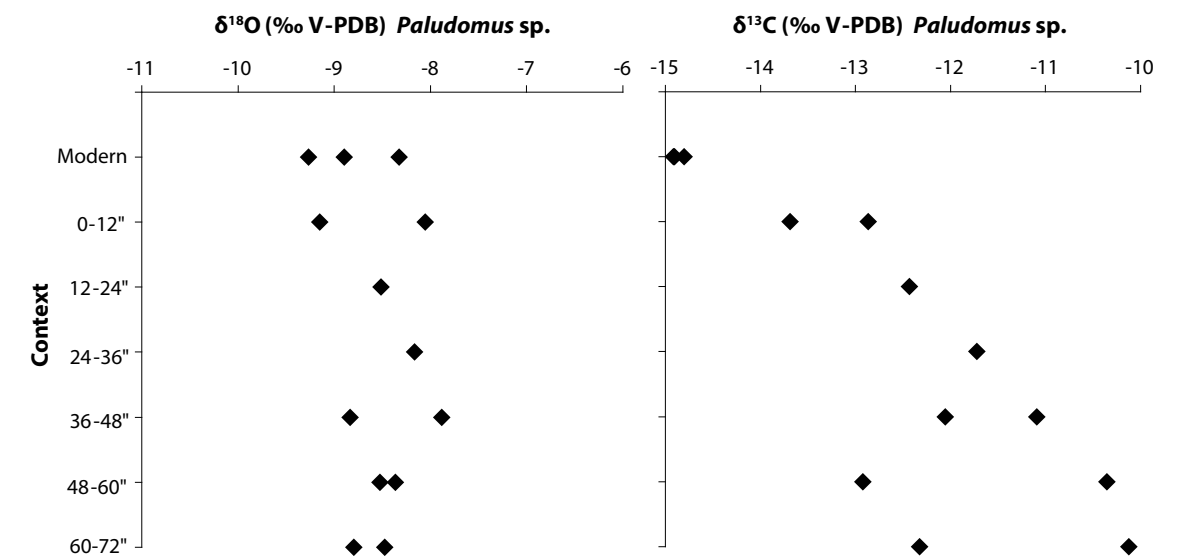


Figure 9.18. $\delta^{18}\text{O}$ and $\delta^{13}\text{C}$ of half-shell analyses of *Paludomus sp.* from successive spit-depths of Trench E/A (samples from the Harrison Excavation Archive). Half-shell analyses of three modern *Paludomus sp.* shells (collected live in April 2002) are shown for comparison.

ranges in $\delta^{18}\text{O}$ than those found in modern specimens whereas similar ranges in $\delta^{13}\text{C}$ exist between the pre-historic and modern shells. All of the prehistoric shells exhibit relatively similar ranges of $\delta^{18}\text{O}$ between the different spit-depths of their respective excavation contexts. Shells of *Geloina erosa* from X/V1 have $\delta^{18}\text{O}$ values that lie between -8.1 to -6% , shells of *Bellamyja javanica** from X/V1 have values that lie between -9.6 to -8.2% , shells of *Bellamyja javanica** from the NCP excavations have $\delta^{18}\text{O}$ values that lie between -9.6 to -8.1% , shells of *Neritina zigzag* from E/A have values that lie between -9.2 to -7.9% , shells of *Paludomus* sp. from E/A have $\delta^{18}\text{O}$ values that lie between -9.2 to -7.9% and shells of *Geloina erosa* from E/G3 have $\delta^{18}\text{O}$ values that lie between -10.4 to -6.8% . There exist similar ranges of $\delta^{18}\text{O}$ values (-9.6 to -8.2% and -9.6 to -8.1% , respectively) between shells of *Bellamyja javanica** from X/V1 and those excavated from NCP Lithofacies 4, although the X/V1 shells exhibit a slightly lighter range of $\delta^{13}\text{C}$ values (-13.9 to -11.9%) than those from the NCP excavations (-13.4 to -11%) (Fig. 9.19).

Preliminary AAR analysis of *Bellamyja javanica** shells from X/V1 indicates periods of harvesting and subsequent deposition of the shells in the West Mouth from the Early Holocene through to the Mid Holocene, and that of *Bellamyja javanica** shells from the uppermost 30 cm of Lithofacies 4 indicates periods of harvesting and subsequent deposition from the Early-Mid to Mid Holocene (Chapter 15). Preliminary AAR determinations on two *Geloina erosa* shells from levels 24-36" and 0-12" of X/V1 indicate harvesting in the Early and Mid Holocene, respectively. During the Mid Holocene back-swamp mangroves reached the northern margins of the Great Cave (Hunt & Rushworth 2005b) and may have promoted the harvesting and subsequent deposition of shells by people using the Great Cave at that time.

Lighter $\delta^{18}\text{O}$ of stream, river and estuary waters might be expected for this time period in Southeast Asia given the Early Holocene maximum in summer monsoon precipitation and the resultant 'amount effect' predicted by climate models (Kutzbach 1981). In addition, higher than modern levels of runoff have also

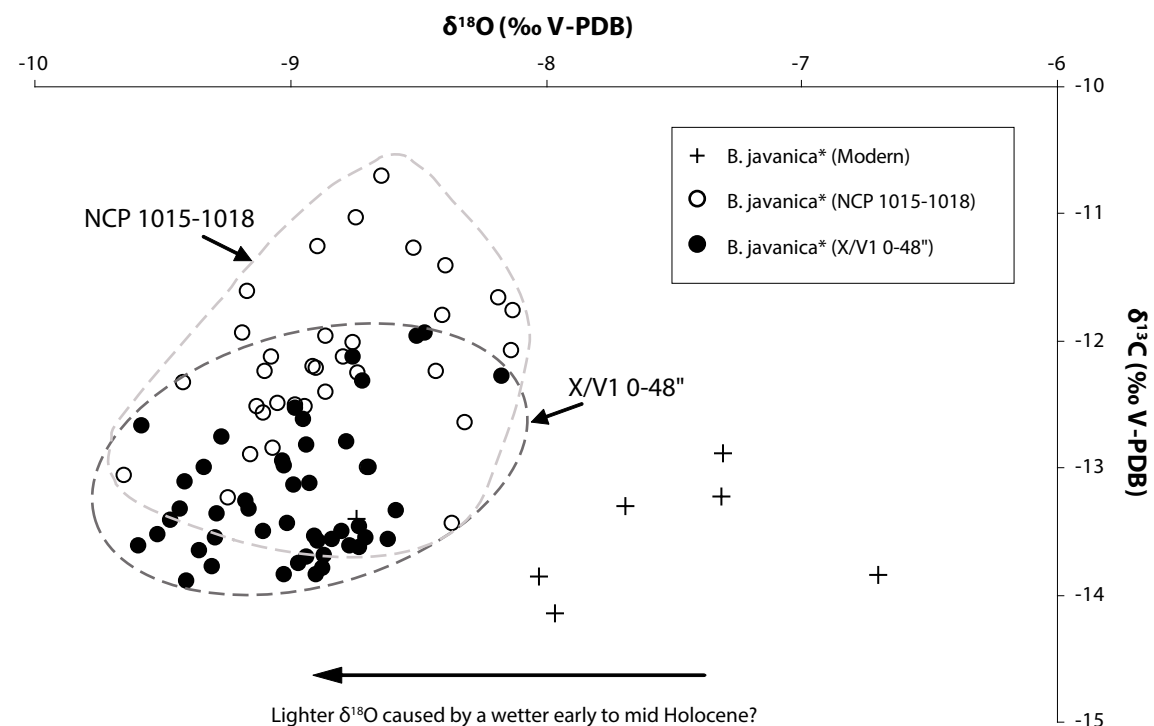


Figure 9.19. Bi-plot of $\delta^{18}\text{O}$ vs. $\delta^{13}\text{C}$ for whole-shell analyses of *Bellamyja javanica** shells from the NCP excavations, Harrison Trench X/V1 and modern comparatives. Note the close similarity in the range of $\delta^{18}\text{O}$ values between the shells analysed from NCP and X/V1. The asterisk by *Bellamyja javanica* denotes that, although this snail was identified as *Bellamyja javanica* following information in the Natural History Museum, London, and Medway (1960a), the detailed re-assessment of the material by Katherine Szabó suggests that it is more likely to be *Cipangopaludina cf. chinensis*.

been interpreted for the Early Holocene in north Borneo from more negative $\delta^{18}\text{O}$ seawater values (lower salinity) in the southern South China Sea (Steinke *et al.* 2006). More negative $\delta^{18}\text{O}$ of rainfall and relatively wetter conditions are also indicated for the Early-Mid to Mid Holocene from speleothem records from Gunung Buda National Park ~100 km ENE of Niah, thought to be in response to the southward shift of the Intertropical Convergence Zone (ITCZ) crossing the equatorial west Pacific (Partin *et al.* 2007). Past changes in temperature can also affect the fractionation of $\delta^{18}\text{O}$, but foraminiferal analyses from sediment cores in the southern South China Sea suggest approximately similar temperatures to those of today during the Early and Mid Holocene (Steinke *et al.* 2006).

The lighter $\delta^{13}\text{C}$ ranges of the prehistoric estuarine shells may also be due to a greater annual surplus of rainfall and reduced salinity in the estuary. The heavier $\delta^{13}\text{C}$ ranges of the prehistoric freshwater may also be explained by increased rainfall that would enhance weathering of limestone bedrocks in the Niah catchment (Stephens & Rose 2005). *Bellamyja javanica* inhabits streams that cut into the limestone bedrock at Niah and would be more susceptible to increased dissolution rates of limestone and heavier $\delta^{13}\text{C}$ stream values as a result. Higher weathering rates have also been reported for the Early Holocene from mineralogical studies of sediments of the Ganges and Brahmaputra Rivers in India (Heroy *et al.* 2003). The recent anthropogenic effect must also be taken into consideration, although this only accounts for ~0.5‰ lighter $\delta^{13}\text{C}$ values (Quay *et al.* 1992).

The reduced amplitude of variation in $\delta^{13}\text{C}$ in the prehistoric estuarine shells of *Geloina erosa* (X/V1) in comparison with modern shells is possibly related to a subdued El Niño Southern Oscillation (ENSO) as indicated in the Early to Mid Holocene from several proxy records across the tropical Pacific region (Donders *et al.* 2008; Gagan *et al.* 2004; and references therein). Such reduced amplitudes of intrashell $\delta^{13}\text{C}$ records in shells of Early and Mid Holocene age in comparison with modern shells have also been documented from coastal southern Peru (Carré *et al.* 2005). The reduced amplitude of variation in $\delta^{18}\text{O}$ in the prehistoric freshwater shells of *Bellamyja javanica** (X/V1 and NCP) may also be related to less variable El Niño events during the Early to Mid Holocene. It is not clear why there are not similar extents of variability in $\delta^{13}\text{C}$ and $\delta^{18}\text{O}$ within shells of *Geloina erosa* and *Bellamyja javanica**; it may be due to particular differences between the estuarine and freshwater zones that they inhabit, such as salinity. The relatively small variations in $\delta^{18}\text{O}$ between spit-depths for each of the prehistoric taxa also indicate that the shells were collected during

a period of less variable palaeoclimatic-hydrological conditions, perhaps associated with a subdued ENSO.

Although similar stable isotopic trends are found between the dated shells from X/V1 and those from E/G3 and E/A, a dating programme of individual shells from the latter two is required in order to place the data into a chronological and regional palaeoclimatic context. The absence of adjacent sections in the field for Trenches E/G3 and E/A removes the possibility of tracing sedimentary layers to the dated strata of Lithofacies 2 and 2C.

The almost identical range of $\delta^{18}\text{O}$ values exhibited between shells of *Bellamyja javanica** from Trench X/V1 and *Bellamyja javanica** shells from the NCP excavations may also indicate, in addition to the AAR determinations, that the proposed correlation of Trench X/V1 with the remaining deposits and radiocarbon age of Lithofacies 4 is sound (Chapter 15). It is interesting to note that no *Bellamyja javanica** shells were found below 48" of X/V1; they may have formed part of the darker brown horizon at the top of Lithofacies 4 from where *Bellamyja javanica** shells were found in the NCP excavations (Fig. 9.6). The darker brown colour of this horizon indicates increased decay of organic (humic) products, probably as a result of increased human activity at this time (Rosenfeld 1964). The generally heavier range of $\delta^{13}\text{C}$ values found in the shells excavated by the NCP team may be the result of local factors, as suggested above.

Laser ablation and drilling analyses of growth profiles of *Geloina erosa* shells from X/V1 and E/G3, respectively, revealed 'saw-tooth' shape cyclical shifts in $\delta^{18}\text{O}$ and $\delta^{13}\text{C}$ (Figs 9.20 and 9.21), as also found in modern specimens (Stephens *et al.* 2008; Fig. 9.2). Unlike their modern counterparts, however, there is a lack of covariation between $\delta^{18}\text{O}$ and $\delta^{13}\text{C}$ in the prehistoric *Geloina erosa* shells from X/V1. The $\delta^{18}\text{O}$ values of the last growth increments of the three midden shells from X/V1 (0-12": -7.4% ; 12-24": -7.1% ; 24-36": -6.9%) are relatively similar to the mean $\delta^{18}\text{O}$ of their corresponding shell profiles (0-12": -6.9% ; 12-24": -7.2% ; 24-36": -7.2%), respectively (Fig. 9.20). The $\delta^{18}\text{O}$ values of the last growth increments of eight of the eleven midden shells from E/G3 (3-6" a: -9.5% ; 6-9" a: -8% ; 6-9" b: -9.7% ; 18-24" b: -9.6% ; 18-24" c: -8.5% ; 60-66": -8.6% ; 66-72" a: -7.7% ; 66-72" b: -8.4%) are relatively similar to the mean $\delta^{18}\text{O}$ of their corresponding shell profiles (3-6" a: -9.5% ; 6-9" a: -8.5% ; 6-9" b: -9.9% ; 18-24" b: -9.1% ; 18-24" c: -8.4% ; 60-66": -8.3% ; 66-72" a: -7.6% ; 66-72" b: -8.8%), respectively (Fig. 9.21). Samples 15-18" (a) and 15-18" (b) have last growth increment $\delta^{18}\text{O}$ values (-8.1% and -7% , respectively) that are heavier than the mean $\delta^{18}\text{O}$ of their corresponding shell profiles (-8.7% and -7.8% , respectively), whereas sample 18-24" (a) has

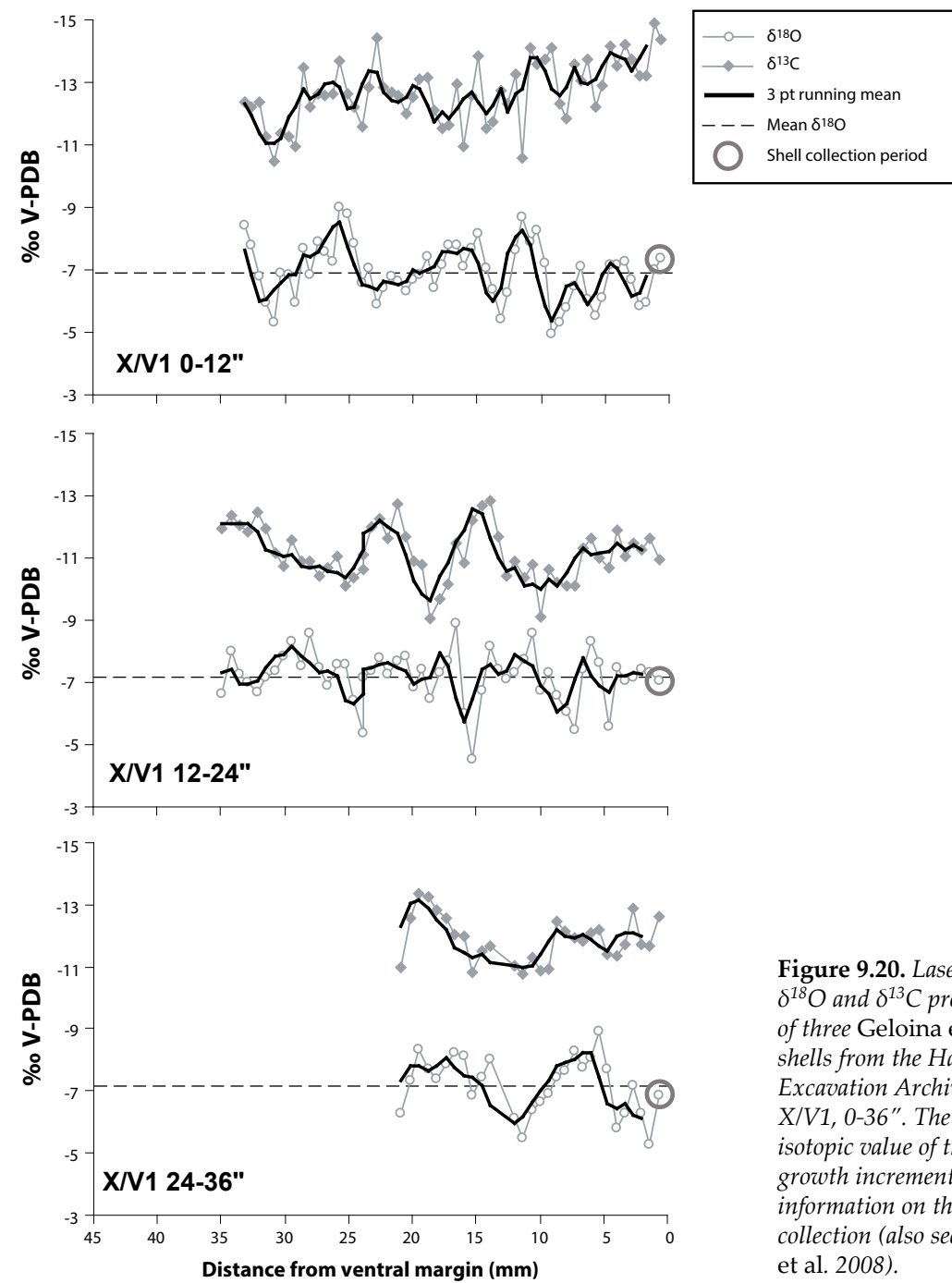


Figure 9.20. Laser ablation $\delta^{18}\text{O}$ and $\delta^{13}\text{C}$ profiles of three *Geloina erosa* shells from the Harrison Excavation Archive Trench X/V1, 0-36". The stable isotopic value of the last growth increment gives information on the timing of collection (also see Stephens et al. 2008).

a lighter last growth increment $\delta^{18}\text{O}$ value (-9‰) than its mean (-8.3‰) (Fig. 9.21).

The similar 'saw-tooth' shape $\delta^{18}\text{O}$ profiles and similar amplitudes of variation in $\delta^{18}\text{O}$ between the prehistoric and modern shells of *Geloina erosa* suggest that broadly similar environmental processes took place in the past as at the present time (Aggarwal et al. 2004). The cyclical shifts in $\delta^{18}\text{O}$ observed in the shells of *Geloina erosa* from X/V1 dating to the Early to Mid

Holocene therefore probably reflect the seasonality of the monsoon rains at these times, with shifts to negative isotopic values the result of high runoff. However, the lack of co-variation between $\delta^{18}\text{O}$ and $\delta^{13}\text{C}$ in the prehistoric shells indicates that the seasonally-large runoff events as inferred from the $\delta^{18}\text{O}$ record do not appear to be in tune with the cyclical shifts of the $\delta^{13}\text{C}$ record. This may be the result of a change in biological processes within the molluscs and because shell $\delta^{13}\text{C}$

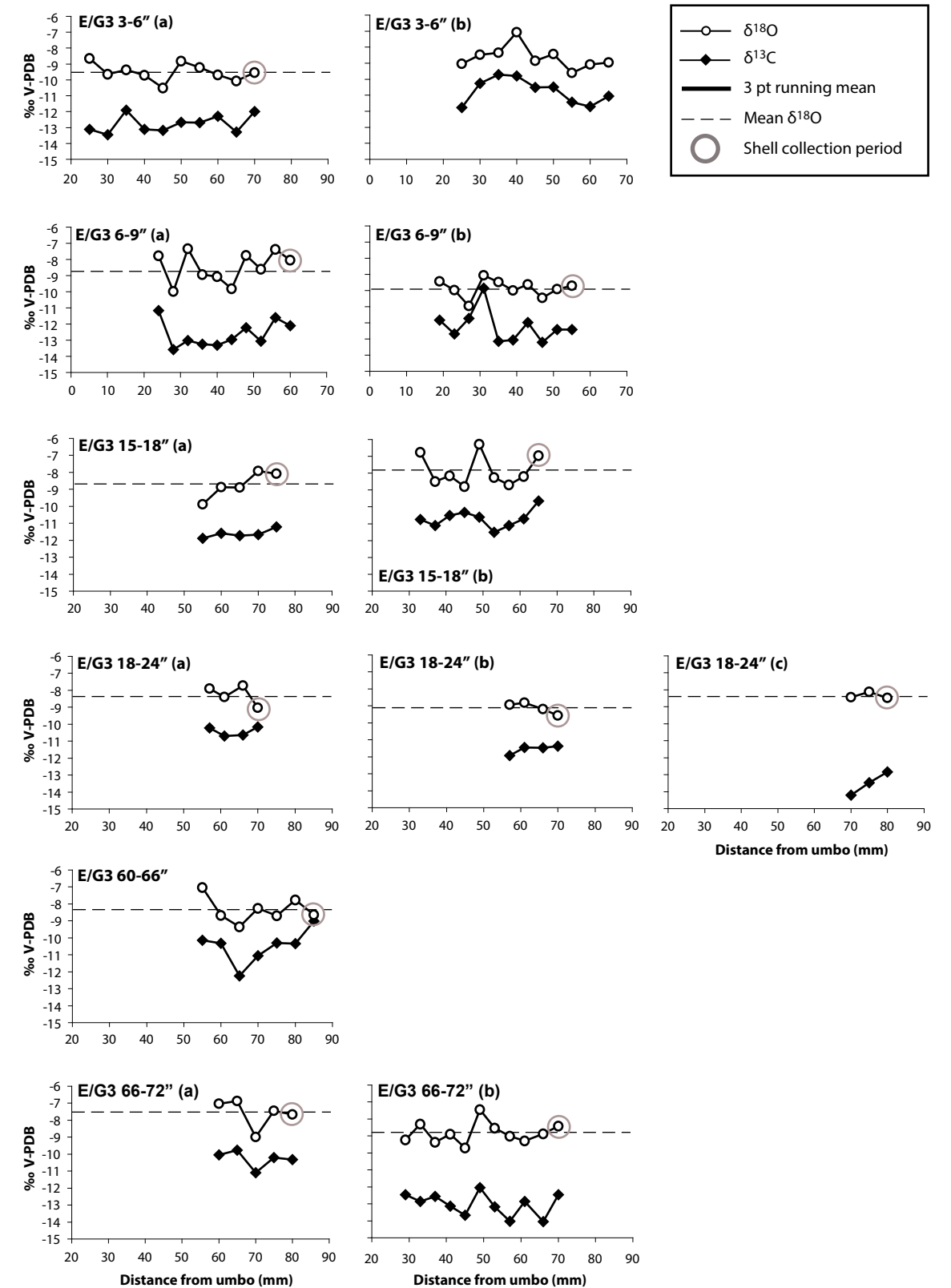


Figure 9.21. $\delta^{18}\text{O}$ and $\delta^{13}\text{C}$ profiles following drilling of *Geloina erosa* shells from Trench E/G3 (samples from the Harrison Excavation Archive). The stable isotopic value of the last growth increment gives information on the timing of collection. Note: the last growth increment of sample 3-6''(b) was not sampled because of shell damage.

variations might be influenced primarily by metabolism rather than the carbon isotopic trend of DIC in the external aquatic environment (Tanaka *et al.* 1986). Palaeoenvironmental interpretation of $\delta^{13}\text{C}$ may therefore be problematic and studies of a greater number of modern *Geloina erosa* shells are obviously required to further understand the factors affecting the $\delta^{13}\text{C}$ signal.

The general similarity between the last growth increment $\delta^{18}\text{O}$ and the mean $\delta^{18}\text{O}$ profile values of the prehistoric shells may indicate that the shells were mostly gathered in times of moderate runoff. Moderate runoff levels may have provided optimal conditions for collecting *Geloina erosa*, as under dry conditions it is known to burrow deeper into mangrove sediments to gain access to groundwater (Morton 1976). Conversely, as our own fieldwork showed, moving through mangroves to gather inter-tidal molluscs can be difficult and sometimes dangerous in the deeper waters during times of high rainfall and flooding.

Conclusion

Although stable isotope analysis is a well-established technique for the analysis of cave deposits, this is the first application of $\delta^{18}\text{O}$ and $\delta^{13}\text{C}$ to midden mollusc shells in Southeast Asia. The isotopic analysis of water samples and modern shells from a range of environmental sub-groups of the Niah catchment revealed similar patterning, with progressive enrichment towards the South China Sea. A close similarity was also found between isotopic shifts in high resolution growth profile analyses of modern *Geloina erosa* shells and variations in recent rainfall. The modern shell and water studies indicate that the modern climate and aquatic environment has a strong control over the stable isotopic signal recorded in the mollusc shells, highlighting the potential of the archaeological material for palaeoenvironmental, palaeohydrological and palaeoclimatic reconstruction. The prehistoric shells of *Bellamyia javanica** and *Geloina erosa* from Harrison's Trench X/V1 in the West Mouth and shells of *Bellamyia javanica** excavated by the NCP team from Lithofacies 4 in Block A, under the rock overhang, both exhibit lighter $\delta^{18}\text{O}$ values than those found in their modern equivalents. These shells have preliminary ages around the Early to Mid Holocene (Chapter 15), when lighter $\delta^{18}\text{O}$ of stream and river waters might be expected in north Borneo as a result of the Early Holocene maximum in summer monsoon precipitation (Steinke *et al.* 2006), as also predicted by climate models (e.g. Kutzbach 1981). Lighter $\delta^{18}\text{O}$ of rainfall and relatively wetter conditions are also suggested for the Early-Mid to Mid Holocene from nearby speleothem records (Partin *et al.* 2007). This indicates that the catchment of the Niah

River was subject to higher rainfall and subsequent higher runoff levels and reduced salinity during the Early to Mid Holocene. The reduced amplitudes of variation in $\delta^{13}\text{C}$ and $\delta^{18}\text{O}$ in prehistoric shells of (respectively) *Geloina erosa* and *Bellamyia javanica** from the West Mouth, in comparison with their modern counterparts, may be related to a subdued ENSO, as indicated in the Early to Mid Holocene from several proxy records across the tropical Pacific region. The similarity of the last growth increment $\delta^{18}\text{O}$ of the prehistoric *Geloina erosa* shells to their mean $\delta^{18}\text{O}$ profile values suggests that these molluscs were gathered by people during times of moderate runoff, in accord with our own experience of the optimal conditions for gathering molluscs in the Niah waters.

Acknowledgements

This project was funded primarily through the main grants to the Niah Caves Project from the Arts and Humanities Research Council, and the AHRC support is gratefully acknowledged. We thank Dr Richard Mani Banda of the Geological Survey of Malaysia for the informed first reconnaissance of the Kuala Niah and its molluscs and are indebted to the late Edmund Kurui (Assistant Curator, Sarawak Museum) for his great skill and endeavour in the field, not least in guiding our collecting work in the estuary and in its fringing mangroves and for obtaining rainfall data for Niah. Melanie Leng and Carol Arrowsmith (NERC Isotope Geosciences Laboratory, Nottingham) are thanked for assistance and kind use of their stable isotope facility. Melanie Leng is also thanked along with Neil Roberts (University of Plymouth) for useful comments on the intrashell stable isotopic data of *Geloina erosa*. David Lowry and Darren Gröcke are thanked for help with stable isotope analyses in the Department of Earth Sciences (RHUL). Thanks are extended to Neil Holloway for help preparing the shells of *Geloina erosa* for laser ablation analysis and thin sectioning in the Department of Earth Sciences (RHUL). Rangkaian Hidrologi Sarawak provided the rainfall data and the Meteorological Service of Malaysia made available the records of temperature and relative humidity. John Taylor and Fred Naggs (Natural History Museum, London) are thanked for help with the taxonomic identification of mollusc shells, as are John Shimmin and Avril Beauquin for help with refinement of the molluscan identifications. We are grateful to Mike Andrews and David Alderton for help with XRD analysis at the University of Reading and Royal Holloway, University of London, respectively. Finally, we thank John Taylor (Natural History Museum, London) for useful discussions on the identification and ecology of *Geloina erosa*.

Chapter 10

The Atmospheric Environment of the West Mouth and its Human, Geomorphic and Archaeological Implications

Brian Pyatt, Gavin Gillmore, John Grattan, Matthew Ivers, David Gilbertson and Paul Phillips

Introduction

This chapter examines the atmospheric environment of the North Chamber of the West Mouth where the archaeological zone is located, and in particular the likely significance for people using the cave of exposure to the gases ammonia (NH_3) and radon (Rn) and to fine-grained airborne particulates (PM_{10}). Exposure to high concentrations of any of these substances is well known to have adverse effects on human health. Fine-grained particulate aerosols might be created by disturbance to the cave sediment surfaces, as well as by human activities such as fires within and outside the cave. Health effects become particularly marked in confined underground environments, such as within a cave and, potentially, in archaeological excavations within the guano sediments. The main sense on entering the West Mouth is the acrid smell of ammonia from the bird and bat guano, and some of the NCP team experienced a degree of irritation to the eyes, nose, and lungs. Hence, as most data on atmospheric pollutants in South and Southeast Asia derive from above-ground surveys in major industrial regions (Biswas *et al.* 2008), one objective of the NCP environmental programme was to seek to understand how ammonia, radon, and PM_{10} varied through the North Chamber of the West Mouth (the primary archaeological zone) in response to factors such as wind speeds, the distance into the cave, the height above the cave sediment, the depth of confined excavation into the cave sediments, etc. We were also interested in the potential influence of different atmospheric conditions on the activities of invertebrates living in the cave, and in turn the effects of such variations (if they existed) on sediment bioturbation, given for example the observations by Tom Harrison (1966a) (and ourselves) of the burrowing activities of the robber wasp *Sphex diabolicus*, which makes burrows up to 10 mm in diameter in modern and old excavation faces. In addition to

the field studies we undertook reconnaissance-level laboratory simulations using different materials, and different but related organisms, to those present in the cave today.

Ammonia

Ammonia is a constituent of the atmosphere, the result of the decomposition of organic materials, as well as of human activities such as fuel combustion. The 'normal' atmospheric concentration in the modern atmosphere is $\sim 20\mu\text{g}/\text{m}^3$ (milligrams per cubic metre) or 0.3–0.6 ppm (parts per million) (Miner 1969). Unlike in the external atmosphere beyond the cave, the distinctive, acrid smell of this colourless gas is immediately evident on entering the West Mouth. This is a familiar property of many caves in the humid tropics, where the gas is mainly a consequence of the process of ammonification of nitrogenous materials such as the urea and the new guano that rain downwards to the cave sediment surface from the bats and birds. Organic nitrogen in these droppings in the form of proteins (amino acids) is converted by micro-organisms such as fungi and nitrogen-fixing bacteria into ammonia (NH_3) and ammonium (NH_4^+). Ammonia production reflects not only the magnitude of these inputs, but also environmental conditions. The presence of higher temperatures and/or the enhanced presence of water at the sediment surface, both features of caves in the lowland hot and humid tropics, will encourage such micro-organisms, and hence the liberation of ammonia into the atmosphere. Ammonia may be dispersed and diluted by winds introducing air through the cave entrances.

Ammonia concentrations in the atmosphere of the northern chamber of the West Mouth were determined initially using a Draeger tubesTM and then more precisely with a DraegerTM portable monitoring system which was calibrated against known concentrations of ammonia before